

---

[All ETDs from UAB](#)

[UAB Theses & Dissertations](#)

---

2016

## Elucidating the Role of the Pro-Survival to Pro-Death Molecular Switch in the IRE1a Signaling Pathway in *Arabidopsis thaliana*

Marie Vollmer Alexander  
*University of Alabama at Birmingham*

Follow this and additional works at: <https://digitalcommons.library.uab.edu/etd-collection>

---

### Recommended Citation

Alexander, Marie Vollmer, "Elucidating the Role of the Pro-Survival to Pro-Death Molecular Switch in the IRE1a Signaling Pathway in *Arabidopsis thaliana*" (2016). *All ETDs from UAB*. 992.  
<https://digitalcommons.library.uab.edu/etd-collection/992>

This content has been accepted for inclusion by an authorized administrator of the UAB Digital Commons, and is provided as a free open access item. All inquiries regarding this item or the UAB Digital Commons should be directed to the [UAB Libraries Office of Scholarly Communication](#).

ELUCIDATING THE ROLE OF THE PRO-SURVIVAL TO PRO-DEATH  
MOLECULAR SWITCH IN THE IRE1A SIGNALING PATHWAY IN *ARABIDOPSIS*  
*THALIANA*

by

MARIE VOLLMER ALEXANDER

DR. KAROLINA MUKHTAR, COMMITTEE CHAIR  
DR. SHAHID MUKHTAR  
DR. ZSUZSANNA BEBOK  
DR. DENISE MONTI

A THESIS

Submitted to the graduate faculty of The University of Alabama at Birmingham,  
in partial fulfillment of the requirements for the degree of  
Master of Science.

BIRMINGHAM, ALABAMA

2016

ELUCIDATING THE ROLE OF THE PRO-SURVIVAL TO PRO-DEATH  
MOLECULAR SWITCH IN THE IRE1A SIGNALING PATHWAY IN *ARABIDOPSIS*  
*THALIANA*

MARIE VOLLMER ALEXANDER

BIOLOGY

ABSTRACT

In eukaryotic cells, the accumulation of unfolded or misfolded proteins in the endoplasmic reticulum (ER) results in ER stress that induces a cascade of reactions termed the unfolded protein response (UPR). The most conserved UPR sensor amongst eukaryotes, Inositol-Requiring Enzyme 1 (IRE1), responds to ER stress by activating a pathway that, under normal conditions, would up-regulate the cellular pro-survival pathway. However, under extreme conditions the infected portion of the plant will ultimately “switch” from pro-survival to pro-death in order to avoid further unfavorable circumstances for the plant as a whole. Arabidopsis possesses two homologs of the major UPR sensor, IRE1a and IRE1b. In this study, I focused on the IRE1a response pathway and the essential role it plays in the immune response of the plant. Unlike mammals, the molecular mechanisms for turning off the pro-survival branch of IRE1a in plants remain largely undefined. In Arabidopsis, IRE1a directly cleaves bZIP60 (basic leucine zipper 60 transcription factor) mRNA in response to both physiological stresses and pathological perturbations, leading to the production of an active transcription factor that promotes the expression of multiple ER stress-responsive genes. Throughout this study, the plant bacterial pathogen *Pseudomonas syringae* pv. *maculicola* ES4326 (*Psm* ES4326) was used as a biotic inducer for ER stress in an attempt to uncover regulatory mechanisms governing bZIP60 expression. We suggest that novel *Arabidopsis thaliana* microRNA (miR5658;

At4g39838) that can potentially target bZIP60, is specifically up-regulated upon acute ER stress. Moreover, quantification of miR5658 reveals its induction coincides with bZIP60 mRNA suppression suggesting that miR5658 might participate in the exquisite regulation of bZIP60 in a manner reminiscent of the mammalian X-box binding protein 1-miR-30c-2\* regulatory mechanism. We also propose that the central plant immune regulator NPR1 (Non-Expressor of *PR* genes 1) plays an important role in regulating miR5658. Taken together, these results suggest that upon cell death-triggering stimuli, NPR1, via miR5658, may target bZIP60 mRNA to turn off the IRE1a-mediated pro-survival pathway.

Keywords: *Arabidopsis thaliana*, ER stress, Unfolded Protein Response, IRE1a, bZIP60, miR5658, NPR1

## DEDICATION

To my parents, Malinda LaMay and Richard Vollmer, who contributed immensely through the whole of my education with unconditional guidance and assistance; and to my husband, Lewis Alexander III, who provided a foundation of support throughout my masters.

## ACKNOWLEDGEMENTS

I want to thank my committee members: Drs. Karolina Mukhtar, Shahid Mukhtar, Zsuzsanna Bebok, and Denise Monti for their expertise and service during the whole of my research. I would like to acknowledge the funding resources for these projects in all or part: the NSF CAREER Award (IOS-1350244) to Karolina Mukhtar, University of Alabama at Birmingham Faculty Development Grant to Karolina Mukhtar, as well as the University of Alabama at Birmingham Department of Biology. I would also like to thank the senior-most members of the Karolina Mukhtar lab: Dr. Camilla Kørner, Xiaoyu Liu, and Dr. Xinran Du for their guidance and advice, and for always being open to listen to questions. Additionally, I would like to acknowledge all of the members of both Mukhtar labs and the UAB Biology Department who assisted me on various projects and gave their time towards making my research project successful.

## TABLE OF CONTENTS

	<i>Page</i>
ABSTRACT .....	ii
DEDICATION .....	iv
ACKNOWLEDGMENTS .....	v
LIST OF TABLES.....	vii
LIST OF FIGURES .....	viii
LIST OF ABBREVIATIONS .....	x
GENERAL INTRODUCTION.....	1
MATERIALS AND METHODS .....	12
RESULTS .....	25
FUTURE DIRECTION.....	38
DISCUSSION.....	39
LIST OF REFERENCES .....	47
APPENDIX A.....	52

## LIST OF TABLES

<i>Table</i>		<i>Page</i>
1	Details of At4g39838 and At4g39840 .....	13

### APPENDIX A

S1	Primers .....	52-55
S2	Primer Color Code.....	55



## LIST OF FIGURES

<i>Figure</i>	<i>Page</i>
1	The zig-zag model of defense ..... 3
2	A model of Arabidopsis IRE1a-mediated Pro-Survival to Pro-Death Signaling Pathways ..... 5
3	Hypothesis- a proposed model for IRE1a Signaling Pathway in Arabidopsis .....7
4	Syringe hand infiltration of <i>Psm</i> ES4326 on Arabidopsis ..... 13
5	Representative bacterial growth on Kb-S media for pathogen infection assay .... 14
6	Mutagenesis Primer Design ..... 22
7	miR5658 is upregulated during cell death induced by <i>Psm</i> ES4326 ( <i>avrRpm1</i> )...25
8	Transcript accumulation of bZIP60 and miR5658 ..... 27
9	Homozygosity Analysis..... 28
10	Bacterial log growth quantification of Arabidopsis ..... 30
11	$\beta$ -glucuronidase (GUS) assay results from WT plasmid .....31
12	$\beta$ -glucuronidase (GUS) assay replicates ..... 32
13	35S:bZIP60-GUS (WT), 35S:bZIP60-GUS (M1) and 35S:bZIP60-GUS (M2) infiltration MUG Assay of Col-0 plants.....34
14	35S:bZIP60-GUS (WT) infiltration MUG Assay of Col-0, <i>npr1</i> , and <i>mel</i> lines.....35
15	Col-0 miR5658 quantification comparing pathogen stress to harmless MgCl <sub>2</sub> ....36

## APPENDIX A

S1	At4g38940/At4g39838 primer and T-DNA insertion design for miR5658.....	56
S2	Position Key for genotyping gel.....	57
S3	Bacterial log growth quantification of Wild-type (WT) Col-0 and mutant plant <i>npr1</i> .....	58

## LIST OF ABBREVIATIONS

BiP2	luminal binding protein 2
<i>bip2</i>	mutant Arabidopsis plant lacking functional <i>BiP2</i> gene
bZIP60	basic leucine zipper 60 transcription factor
<i>CAM</i>	calmodulin
cDNA	complementary DNA
Col-0	Columbia-0
<i>CRT</i>	calreticulin
EDR	enhanced disease resistance
ER	endoplasmic reticulum
ETI	effector-triggered immunity
IRE1a	Inositol-Requiring Enzyme 1a
<i>mel38</i>	miR5658 expressing line for At4g39838 mutant line
<i>mel40</i>	miR5658 expressing line for At4g39840 mutant line
<i>mel38/40</i>	miR5658 expressing line for At4g39838/At4g39840 mutant line
miR5658	microRNA-5658
PTI	pathogen-triggered immunity
NPR1	Non-expresser of <i>PR</i> genes 1
<i>npr1</i>	immuno-compromised mutant Arabidopsis plant lacking functional <i>NPR1</i> gene
PAMPs	pathogen-associated molecular patterns
PCR	polymerase chain reaction

<i>PDI</i>	protein disulphide isomerase
PR	pathogenesis-related
PRR	pattern recognition receptors
<i>Psm</i> ES4326	<i>Pseudomonas syringae</i> pv. <i>maculicola</i> strain ES4326
<i>Psm avrRpm1</i>	avirulent bacterial strain <i>Psm</i> ES4326 carrying <i>avrRpm1</i> effector
R protein	resistance protein
RIDD	regulated IRE1-dependent decay of mRNA
RT-PCR	reverse transcriptase polymerase chain reaction
RT-qPCR	real-time quantitative polymerase chain reaction
SA	salicylic acid
SAR	systemic acquired resistance
RISC	RNA-induced silencing complex
TF	transcription factor
UPR	unfolded protein response
WT	wild type

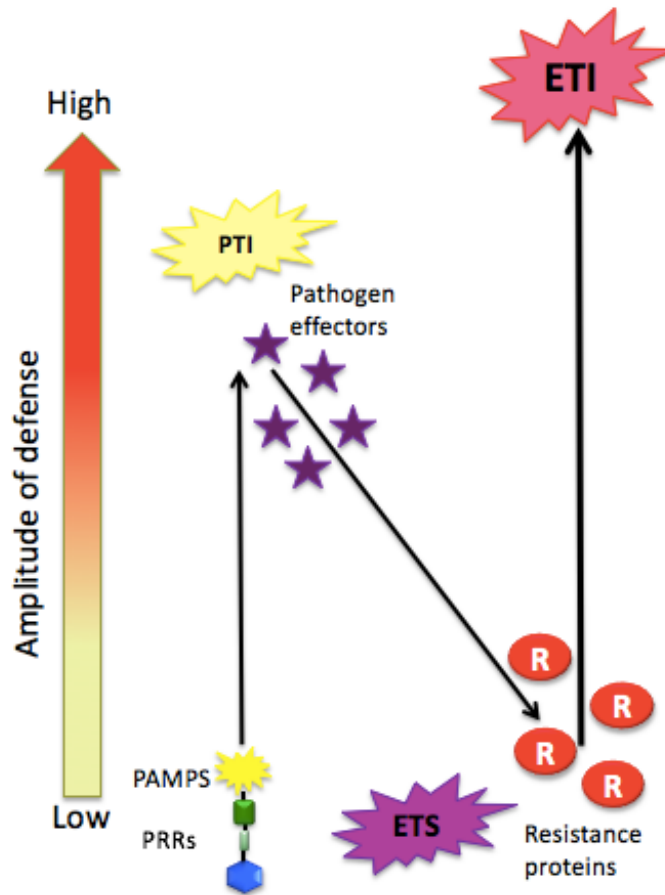
## **GENERAL INTRODUCTION**

Plants are involved in a perpetually complex battle for dominance with their pathogens (Dodds and Rathjen 2010). The struggle between plants and pathogens sparked intense investigation amongst the world's scientists and researchers to understand the regulatory mechanisms involved in both players. Nearly half of the plant population is threatened due to various eradicating factors including abiotic and biotic factors, and the effect of this on the human population is not entirely unknown (Nilsen et al., 1996). Plants are subjected to climate associated stress, habitat depletion, and attacks via biotic factors including fungi, viruses, bacterial pathogens, among other stressors (Nilsen et al., 1996). And while the plant population is under pressure, there is a reciprocal effect concerning the human population and this may very well yield the completion of both populations simultaneously. The World Bank estimates there are around 7.125 billion people on earth and rising (Population, total. World Bank). Considering that our primary food source is the plant population, the escalating matters pressuring their population and how plants react to them is the focus of plant research. The reciprocal effect of the plant to human population has prompted a growing interest among scientists around the world to understand the plant defense response. As a result of the issues threatening our primary food source, would not the elucidation of how plants manage destructive and/or stressful conditions be imperative for the plants survival, as well as our own? Accordingly, we seek to understand the cellular regulatory mechanisms governing a specific plant defense pathway, the IRE1a pathway.

## **The battle for dominance**

The pronounced appearance of pathogen stress upon plants sparked a co-evolutionary battle for dominance between the two millions of years ago. This battle is never “one-and-done”, with one of the two winning at the initiation of first contact, but rather it is a progressive molecular tug-of-war that depends on the internal network of organelles, enzymes, receptors, specialized secretory cells, and other key players in both plant and pathogen (Nimchuk et al., 2003). Plants have an amazing ability to recognize pathogen attack through methods involving both conserved and variable pathogen receptors, and pathogens can manipulate the plant defense response through secretion of virulence effector proteins (Dodds and Rathjen 2010). Plants have endured the stated necessity of fighting for survival, and undeterred by the battle, they have evolved a highly sophisticated innate immune system to inhibit pathogen invasion and multiplication (Jones and Dangl 2006). At the beginning of contact of pathogen to plant, the pathogen will attempt to infect the plant at the same time the plant recognizes the attack has happened. The molecular tug-of-war between plant and pathogen is demonstrated by the zig-zag model of defense (Fig.1). Pathogens have pathogen-associated molecular patterns (PAMPs) which are can be recognized by a specific plant receptor, namely the pattern-recognition receptors (PRRs) (Jones and Dangl 2006). Once the PRRs recognize an attack, they initiate the commencement of the molecular tug-of-war. The first level of defense from the plant is characterized as pathogen-triggered immunity (PTI) and is notorious for being a mild form of defense (Bigeard et al., 2015). After PTI is triggered, the pathogen can fight back by inserting effector proteins into the plant cell in order to block the PTI.

Effector proteins lead to victory for the pathogen known as effector-triggered susceptibility (ETS). Despite this, the tug-of-war is not over. The plant can express resistance (R) proteins to hinder the effect of effector proteins leading to a higher level of defense for the plant or effector-triggered immunity (ETI) (Tsuda and Katagiri 2010).

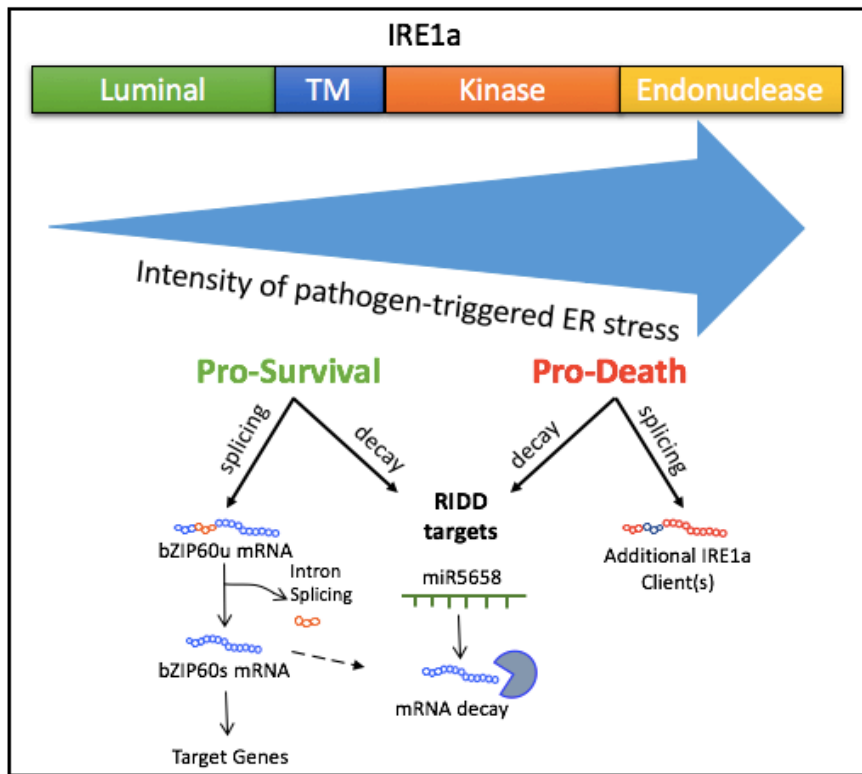


**Figure 1. The zig-zag model of defense.**

Furthermore, in response to pathogen attack, the plant innate immune system can induce long lasting and broad-spectrum enhanced resistance known as systemic acquired resistance (SAR). SAR is activated by the accumulation of the immune signal phytohormone salicylic acid (SA), which results in an increase in production of pathogenesis-related (PR)-proteins with antimicrobial properties (Anand et al., 2008).

NPR1 is identified as the major transcriptional regulator of SA-mediated defense response (Wu et al., 2012). SA will act as a signaling molecule devoted to various plant defense pathways against biotrophic and hemibiotrophic pathogens (Boatwright 2013). Upon pathogen attack, the level of SA will increase at the site of infection, and by way of an unknown signal, the increasing level of SA will extend through the whole of the plant-acting as an alarm for further attacks and initiating SAR. Moreover, SAR induces a large set of ER-resident genes to insure proper folding and secretion of PR proteins (Anand et al., 2008). The goal of these ER-resident genes is to prevent the accumulation of unfolded proteins in the lumen and maintain homeostasis. Under basal conditions, the ER is dedicated to the protein folding process to insure quality control amongst the cell (Fanata et al., 2013). A number of genes in the plant genome encode ER-resident peptides that function to fold proteins for transfer to the Golgi apparatus for further modification and secretion. However, under stressful conditions including pathogen attack, this fool-proof folding process is obstructed and triggers unfolded protein accumulation in the lumen. The initial intent of the unfolded protein response is to ensure cell survival; however, under severe or prolonged ER stress it will rewire cellular signaling and eventually trigger cell death. There are two branches of defensive strategies (Fig 2): safeguard from pathogens by recognition and triggered immunity through bZIP60-dependent splicing (pro-survival) or programmed cell death through bZIP60 degradation via miR5658 (pro-death).





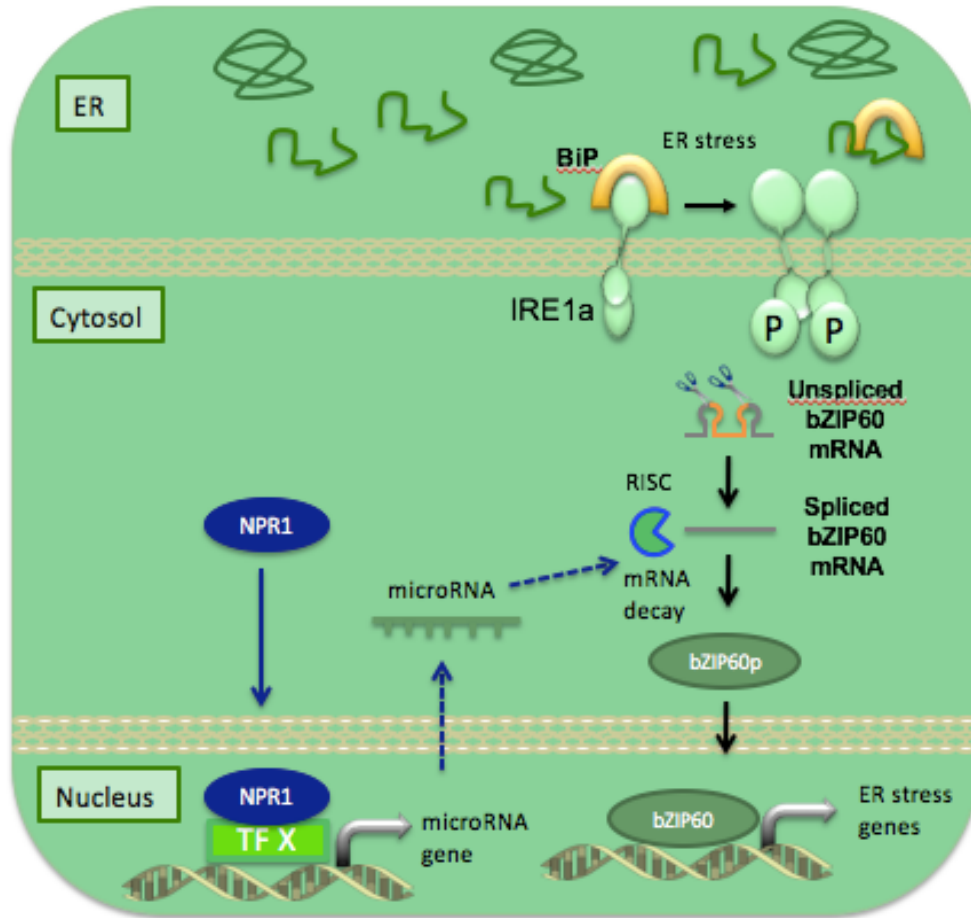
**Figure 2. A model of Arabidopsis IRE1a-mediated Pro-Survival to Pro-Death Signaling Pathways.**

### Understanding how plants handle stress at the molecular level

Environmental and genetic factors that disrupt ER function can cause the accumulation of misfolded and unfolded proteins in the ER lumen, a condition termed ER stress (Oslowski and Urano, 2012). The accumulation of unfolded proteins activates the outset of the unfolded protein response (UPR) to orchestrate the recovery of ER function (Hetz 2012). The UPR is a homeostatic signaling network with the intent to recover cellular stability, though the failure to adapt to ER stress may result in the cell being forced to switch to apoptotic cellular suicide (Hetz 2012). Some ER-resident proteins participate in the UPR, regulated in part by the highly conserved ER membrane bound Inositol Requiring Enzyme 1a (IRE1a). IRE1a is an ER membrane-located kinase/endoribonuclease

enzymatic protein that is suggested to be a key player in the activation of UPR homeostatic restoration (Moreno et al., 2012). Genetic studies of the Arabidopsis BiP2 (luminal Binding Protein 2) suggest that the IRE1a branch of the UPR plays a significant role in plant immunity considering the *bip2* mutant is defective in SAR (Wang et. al, 2005). Further experimentation on this subject provided evidence that IRE1 is directly related to the production of UPR-responsive genes and *PR* genes through the revelation that *ire1* mutants are deficient in their production.

Taken together, the existing experimental evidence suggests that IRE1a is an important regulator of the biotic stress-triggered UPR and SAR (Moreno et al., 2012). IRE1a is a distinguished detector of ER stress because of the position it's two enzymatic domains take in the cell. IRE1a is positioned on the membrane of the ER, with a sensor domain associated with BiP in the luminal side and a kinase and RNase domain in the cytoplasmic side of the cell (Fig.3). The position of IRE1a's enzymatic domains in both ER lumen and cytosol is essential in detecting ER stress and activating a downstream response.



**Figure 3. Hypothesis- a proposed model for IRE1a Signaling Pathway in Arabidopsis.**

We propose that the luminal (sensor) domain senses unfolded proteins via the disassociation of BiP which leads to the activation of IRE1a through oligomerization and trans-autophosphorylation, initiating UPR through the cytoplasmic domain (Fig. 3). The downstream players of the IRE1a signaling pathway, however, have proved to be more difficult to characterize than others. Foregoing research validates our hypothesis that BiP disassociates to initiate the UPR upon ER stress (Srivastava et. al, 2013). Likewise, additional research confirms that IRE1a catalyzes the unconventional, cytoplasmic splicing event of bZIP60 mRNA to produce an active transcription factor (TF) (Nagashima et. al, 2011). In Arabidopsis, IRE1a primarily catalyzes the cytoplasmic splicing of bZIP60

mRNA under mild biotic or abiotic stress conditions (Moreno et al. 2012). The IRE1-bZIP60 signaling pathway is analogous to the IRE1p-HAC1 in yeast pro-survival conditions (Zhang et al., 2015). Both signaling pathways, described in Arabidopsis and yeast, constitute the pro-survival branch of the UPR through the induction of ER-stress relievers. bZIP60, as a key cell fate regulator, is expected to have complex transcriptional and post-transcriptional regulation mechanisms. The spliced bZIP60 transcription factor is predicted to translocate to the nucleus, where it activates the expression of cytoprotective genes that are involved in ER stress relief for the pro-survival branch of the IRE1a signaling pathway. In response to various stressful conditions including pathogen infection, extreme temperature, salicylic acid treatment, tunicamycin, and dithiothreitol, the cytoplasmic splicing of bZIP60 mRNA in plants is catalyzed by IRE1a (Zhang et al., 2015). Splicing eliminates a transmembrane domain within bZIP60 to produce the bZIP60s TF, which in turn upregulates UPR target genes, including *BiP* (coding for luminal binding proteins), *CAM* (calmodulin), *CRT* (calreticulin) and *PDI* (protein disulphide isomerase) (Zhang et al., 2015).

The bZIP60s TF normally promotes expression of cytoprotective genes involved in protein folding or ER stress relief; however, under severe or prolonged stress, we hypothesize that a specific microRNA downstream of the IRE1a-signaling pathway, miR5658, will recruit a protein complex called the RISC (RNA-induced silencing complex), leading to *bZIP60* mRNA decay. MicroRNAs can act as molecular switch in several signaling pathways of the eukaryotic cell because they can control gene expression post-transcriptionally by binding to various mRNAs (Sotiropoulou et al., 2009). We hope to clarify the role of Arabidopsis IRE1a-splicing substrate, bZIP60, as a direct molecular

switch, which targeted by miR5658, will turn off the IRE1a-mediated pro-survival pathway. The question remains exactly *how* the cell switches from cellular survival to apoptosis, and what key players are involved in this mechanism.

### **Small but powerful: MicroRNAs**

MicroRNAs are an abundant class of small non-coding ~20-24 nucleotide RNAs that are involved in various processes within the plant cell (Zhang et. al, 2006). Hundreds of microRNAs with different biological functions are expressed in a plant cell, but the exact biological mechanism of action has only been described for a few. Several groups have recently reported microRNAs present in Arabidopsis, and new numbers are on the rise. Sunkar and Zhu (2004) isolated 21 new microRNAs from Arabidopsis at a time when only 43 microRNAs had been reported, just by constructing an RNA library for experimentation. Additionally, it has been established that microRNAs have numerous important roles in plant post-transcription gene regulation by targeting and binding to mRNAs for cleavage or degradation (Zhang et. al, 2006). A considerable body of evidence has shown that miRNAs play multiple roles in plant biological processes including adaptive responses to diverse abiotic and biotic stresses by negatively regulating their target proteins. In our study, microRNAs are the prime area of interest because of their novel function as a regulator of mRNA degradation in the plant cell. MicroRNAs function by the incorporation of themselves into the RISC, and then consecutively annealing to another RNA molecule with a complementary sequence. Only one strand of the microRNA, the guide strand, is successfully incorporated into the RISC, while the other strand, the passenger strand, is eliminated (Wang 2010). Accordingly, single stranded

microRNA in the RISC can bind to specific target sequences within the coding region of mRNA transcripts (Dalmay 2013). This gives microRNAs the ability to “guide” the RISC to mRNA transcripts for silencing or degradation. We predict that a specific microRNA, miR5658, will target the *bZIP60* mRNA transcripts upon acute ER stress to transition the cell into apoptosis (Fig. 2). In this project, I studied miR5658 targeting bZIP60 spliced mRNA and the initiation of the pro-death branch. I set out to determine the specific activity of miR5658 on bZIP60 regulation *in planta*.

### **NPR1 as a regulator for miR5658 expression**

In addition to the plant immune players introduced above, we have also found from preliminary research and experimentation that the central plant immune regulator NPR1 (Non-expresser of *PR* genes 1) may play an important role in the IRE1-mediated defense pathway by regulating the expression of miR5658. NPR1 has long been known as a master co-regulatory protein involved in plant immunity. It has been well documented that NPR1 is involved in the plant defense response, and a recent report also proposed that it may function as a key receptor for SA (Wu et al., 2012). NPR1 has been characterized as fundamental to the activation of the SA-dependent plant defense pathway in SAR (Wu et al, 2012). This is a significant uncovering of NPR1’s involvement, because it directly portrays the role NPR1 plays in the plant innate immune system. In this dissertation, I propose that NPR1 plays a novel, previously unexplored role in plant immunity. A transgenic NPR1 Arabidopsis plant, known as *npr1*, has been artificially immunocompromised via loss-of-function NPR1 to generate an incomparable disease susceptible plant. We have hypothesized that *npr1* plants may hyper-activate the

expression of miR5658 but lost the ability to induce it because NPR1 is absent to regulate the expression. Also, we propose that because NPR1 is absent in the cell, the *npr1* plant chooses to hyper-activate miR5658 which may be a key player in the apoptotic branch of the IRE1a-mediated defense pathway. In this dissertation, I present evidence linking NPR1 with accumulation of miR5658 and bZIP60 transcript levels.

## **MATERIALS & METHODS**

### **Plant Growth Conditions**

For the protein, DNA and RNA sampling and pathogen infections, seeds were sown on MetroMix 360 soil and incubated for 72 h at 4°C. Seeds were then transferred to a growth room (12 h light/12 h dark) at 65% humidity for two weeks. Seedlings were transplanted into 72 well trays and continued growing for two additional weeks at growth room conditions before treatments.

### **Homozygous *mel* mutant confirmation**

Three different Arabidopsis T-DNA insertion mutant lines for miR5658 were isolated from the SALK collection to knock out individual locus or both loci in order to prepare transgenic plants which do not express miR5658 (Supplemental Figure 1, see Appendix). From those, I developed homozygous loss-of-function miR5658 Arabidopsis mutants through genotyping polymerase chain reaction (PCR) and confirmation of the PCR results using agarose gel electrophoresis. The primer pairs (included in appendix A) were synthesized for miR5658: At4g39840 and At4g39838 because of their locus overlap. These homozygous transgenic lines have been named *mel* (for *microRNA expressing line*), specifically *mel38*, *mel40*, and *mel38/40* (At4g39838, At4g39840, At4g39840/At4g39838 respectively) corresponding to the gene that they are homozygous for.



Locus Overlap	
At4g39840	At4g39838
Molecular Function Unknown	Potential Natural Antisense Gene
Biological Process Unknown	
Located in Endomembrane System	

**Table 1. Details of At4g39838 and At4g39840.**

### Pathogen Treatment

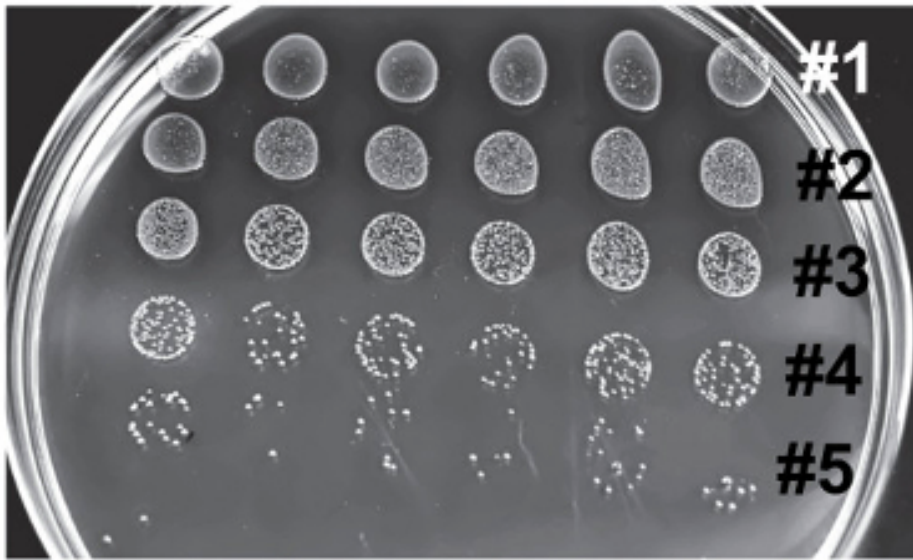
#### Bacterial Inoculation Procedure



**Figure 4. Syringe hand infiltration of *Psm* ES4326 on Arabidopsis.**

Infection of Arabidopsis plants with *Pseudomonas syringae* pv. *maculicola* (*Psm*) ES4326 was performed on four-week-old plants. To test for enhanced disease resistance (EDR), a bacterial suspension of  $OD_{600} = 0.001$  was hand infiltrated into two leaves per plant and 12 plants/genotype. Sampling in EDR required the removal of two 6-mm leaf discs per plant from six to twelve plants three to four days post inoculation. Two leaf discs per genotype/treatment were placed in 500  $\mu$ L of 10 mM  $MgCl_2$  and homogenized to break open the plant tissue and release the bacteria. Aliquots of 20  $\mu$ L were taken from each homogenized mixture and placed into a 96-well plate containing 180  $\mu$ L of  $MgCl_2$  per well. Serial dilutions (1:10) were made from the first row down to the sixth row by removing 20

$\mu\text{L}$  from each preceding well to the one beneath it. These dilutions were all plated onto KB media containing streptomycin antibiotics. Each genotype is grown on separate Kb-S media in order to differentiate growth patterns and convert those to a graph for analysis. Bacterial growth is quantified 3 days later.



**Figure 5. Representative bacterial growth on Kb-S media for pathogen infection assay.** Numbers 1-5 represent serial dilutions of the same genotype. Image adopted from (Liu X.... Vollmer M. JoVE 2015)

## **Plant Molecular Procedures**

### **Quick Genomic DNA Extraction for Genotyping**

Two leaves from 4-week old Arabidopsis plants were mashed into a 96-well plate using Fisherbrand 1-200 $\mu$ L beveled pipet tips. The leaves were mashed with 0.25 M sodium hydroxide, 0.25 M hydrochloric acid, and 0.5 M Tris HCl. The product is crude lysate that is suitable for genotyping PCR reaction.

### **Agarose Gel Electrophoresis**

After PCR reaction, electrophoresis was performed on 1% ethidium bromide agarose gels at 80-100 volts. Gels were run on a Bio-Rad PowerPac<sup>™</sup> Basic and imaged using the Bio-Rad Molecular Imager<sup>®</sup> Gel Doc<sup>™</sup> XR+ with Image Lab<sup>™</sup> software. The position of the bands at the completion of the electrophoresis is essential in determining whether the individual is homozygous for the WT allele, heterozygous, or homozygous for the mutant allele.

### **RNA extraction and RT PCR**

Arabidopsis leaves were separated from the stem and harvested in liquid nitrogen and subsequently homogenized using a Fisher Scientific PowerGen<sup>™</sup> High Throughput Homogenizer. RNA extraction was performed using TRIzol reagent (Invitrogen) and followed by treatment with DNase I. TRIzol (1 mL) was added to homogenized tissue samples and briefly vortexed. Samples were incubated for five minutes at room temperature followed by the addition of 0.35 mL of chloroform. Samples were vortexed

again and then centrifuged at 12 krpm for 15 minutes at 4°C. RNA was transferred to another centrifuge tube and precipitated using 650  $\mu$ L of 100% isopropanol. Samples were subsequently incubated at room temperature for 10 minutes and centrifuged at 12 krpm for 10 minutes at 4°C. The resulting RNA pellet was washed with 70% ethanol made with diethylpyrocarbonate (DEPC) water. Samples were then centrifuged at 7.5 krpm for 10 minutes at 4°C. The supernatant was then aspirated and the samples were centrifuged again for 10 seconds to remove remaining droplets. The pellet was dried at room temperature for five to ten minutes and resuspended in 20  $\mu$ L of DEPC water. RNA was then transferred to a PCR strip and diluted with water, DNase buffer and DNase enzyme to a volume of 20  $\mu$ L at 500 ng of RNA per  $\mu$ L. Strips were incubated at 37°C for 25 minutes using an Applied Biosystems Veriti 96-Well Thermal Cycler. DNase was then deactivated with 5  $\mu$ L of Ambion's DNase-free resin suspension. cDNA was synthesized using a SuperScript II first-strand RT-PCR kit (Invitrogen) following manufacturer's protocol.

### **DNA extraction for fresh plant tissue**

Leaf discs (~0.2 g per genotype) were homogenized after treatment with liquid nitrogen. 200 $\mu$ L of DNA extraction buffer and 5 $\mu$ L of RNase I was added to the homogenized tissue and vortexed shortly. The mixture is left at 65°C until the solution turns dark green vortexing every 5 minutes. 200  $\mu$ L of chloroform:isoamyl alcohol was transferred to the mixture and tubes were mixed gently. Samples were centrifuged for 15 minutes at 15 krpm at 4°C. The supernatant was then transferred to 140  $\mu$ L of isopropanol, mixed and incubated for 20 minutes at room temperature. Samples were centrifuged again for 15 minutes at 13.2 krpm at 4°C. The DNA pellets were washed with 500  $\mu$ L of 70%

ethanol (EtOH) for 5 minutes at 13.3 krpm. The EtOH was removed and centrifugation was repeated with 95% EtOH for 1 minute to remove remaining droplets. Samples were air-dried for 5 minutes after which 20  $\mu$ L of dH<sub>2</sub>O was added and samples were stored at 4°C. Samples were analyzed using qPCR, Arabidopsis ubiquitin primers (Guillemette *et al.*, 2004).

### **Quantitative real-time PCR (qPCR) analysis**

The qPCR master mix contained 4  $\mu$ L of nuclease-free water, 2  $\mu$ L forward primer, 2  $\mu$ L reverse primer and 10  $\mu$ L of GoTaq<sup>®</sup> BRYT Green (Promega) per sample. Each reaction well contained 18  $\mu$ L of the corresponding master mix and 2  $\mu$ L cDNA. An Eppendorf realplex<sup>2</sup> Mastercycler<sup>®</sup> was used to measure sample fluorescence. qPCR cycles ran at 95°C for 10 min, followed by 40 cycles at 95°C for 15 seconds, 55°C for 30 seconds and 72°C for 30 seconds. Melt curve ran at 95°C for 15 seconds, 60°C for 15 seconds and increased incrementally to 95°C over 20 minutes. Means and standard errors were calculated from three replicate measurements per genotype per treatment.

### **microRNA qPCR**

RNA extraction was performed as detailed above. Reverse transcription master mix included 0.15  $\mu$ L of 100mM dNTP mix, 4.16  $\mu$ L of nuclease-free water, 1.00  $\mu$ L of multiscribe reverse transcriptase, 1.50  $\mu$ L of 10X reverse transcriptase buffer, 0.19  $\mu$ L of RNase inhibitor, and 3  $\mu$ L of appropriate RT primer provided. Mixture was incubated to 16°C for 30 minutes, and then 30 minutes at 42°C, followed by 5 minutes at 85°C. RT reaction included 10  $\mu$ L of the RT master mix along with 5  $\mu$ L of RNA. qPCR master mix

included 7.67  $\mu\text{L}$  of nuclease-free water, 1.00  $\mu\text{L}$  of TaqMan microRNA assay (20X), 10.00  $\mu\text{L}$  of TaqMan 2X universal PCR master mix, along with 1.33  $\mu\text{L}$  of product from RT reaction. Reaction wells contained 18.67  $\mu\text{L}$  of master mix and 1.33  $\mu\text{L}$  of the RT product. Samples were incubated at 95°C for 10 minutes, followed by 40 cycles of 95°C for 15 seconds and 60°C for 60 seconds. Means and standard errors were calculated from three replicate measurements per genotype.

### **Cloning PCR**

DNA extraction was performed as described above and was mixed in a 96 well plate with 1  $\mu\text{L}$  Forward primer, 1  $\mu\text{L}$  Reverse primer, 12.4  $\mu\text{L}$  nuclease free water, 4  $\mu\text{L}$  5X Phusion HF Buffer, 0.4  $\mu\text{L}$  dNTP, and 0.2  $\mu\text{L}$  Phusion DNA polymerase. The reaction consisted of 1  $\mu\text{L}$  of genomic DNA with 19  $\mu\text{L}$  of master mix. Mixture was incubated to 98°C for 30 seconds, followed by 30 cycles of 5-10 seconds at 98°C, 10-30 seconds at X°C (depending on length of primers see [www.thermoscientific.com/pcrwebtools](http://www.thermoscientific.com/pcrwebtools)), 15-30 seconds (s/kb) at 72°C, and then 5-10 minutes at 72°C.

### **BP Clonase™ Reaction**

5  $\mu\text{L}$  of PCR product from cloning PCR was mixed in an Eppendorf tube with 2  $\mu\text{L}$  of vector pDONR207, 4  $\mu\text{L}$  of BP Clonase™ enzyme mix, 4  $\mu\text{L}$  5X BP Clonase™ Reaction Buffer, and 1  $\mu\text{L}$  of TE Buffer and incubated overnight at 25°C. 2  $\mu\text{L}$  of Proteinase K solution was added to the mixture and incubated for 10 minutes at 37°C.

### **Transformation into competent cells**

1  $\mu\text{L}$  of the BP Clonase<sup>TM</sup> reaction was mixed with 50  $\mu\text{L}$  of competent cells into a new Eppendorf tube and set on ice for 30 minutes. The mixture was then incubated at 42°C for 45 seconds, and then immediately transferred back to ice for 2 minutes. 1 mL of LB broth was added to the mixture and shook at 37°C for 1 hour. The supernatant is discarded and resuspended in 100  $\mu\text{L}$  of leftover LB media and spread onto LB agar plates. Plates are incubated overnight at 37°C. After incubation, a single colony from each sample is subcultured onto a new LB agar plate to generate a plate of growth from one specific colony.

### **MiniPrep Plasmid DNA Preparation**

Growth from LB colony plates was subcultured into LB broth and grown at 37°C in the shaker overnight. Bio Basic EZ-10 Spin Column Plasmid DNA Minipreps Kit was used to perform miniprep before sequencing reaction. 5 mL of overnight culture is added to a 14 mL falcon round-bottom tube and centrifuged at 12 krpm for 2 minutes. The liquid is drained and 100  $\mu\text{L}$  of Solution I from the kit is mixed with the pellet and kept for 1 minute. 1  $\mu\text{L}$  of VisualLyse is added to the mixture. 200  $\mu\text{L}$  of Solution II from the kit is added to the mixture and mixed by inverting the tube 4-6 times. 350  $\mu\text{L}$  of Solution III from the kit is added to the mixture and mixed gently. The mixture is incubated at room temperature for 1 minute. The mixture is centrifuged at 12 krpm for 5 minutes. The above supernatant was transferred to the EZ-10 column and centrifuged at 10 krpm for 2 minutes. The flow-through was discarded and 750  $\mu\text{L}$  of Wash solution with EtOH was added to the column and centrifuged at 10 krpm for 2 minutes. The wash procedure was repeated one time. The

flow-through was discarded and the mixture was centrifuged at 10 krpm for an additional minute. The column is transferred to a 1.5 mL microfuge tube and 50  $\mu$ L of elution buffer is added to the column and incubated at room temperature for 2 minutes. The tube is then centrifuged at 10 krpm for 2 minutes. The purified plasmid DNA was stored at -20°C until sequencing.

### **Sanger BigDye Sequencing**

Sequencing reaction contained 5  $\mu$ L of our purified plasmid DNA with 3  $\mu$ L of 4M betaine, 3  $\mu$ L of nuclease free water, 2.5  $\mu$ L of BigDye Terminator v1.1/3.1 Sequencing buffer (5X), 1  $\mu$ L of specific sequencing reverse and forward primer (Supplemental Table 1, see Appendix), and 1  $\mu$ L of BigDye. The reaction is added to the thermal cycler and incubated at 98°C for 10 minutes, followed by 25 cycles of 10 seconds at 98°C, 5 seconds at 50°C, 4 minutes at 60°C. Samples were submitted to the Heflin Center Genomics Core Lab and data rendered were in fastq format. Fastq files were used to produce both .bam and .bai files so that data could be visually examined using the ApE (A plasmid Editor) website for sequence files.

### **Site-directed mutagenesis PCR (protocol adapted from Stratagene)**

Plant DNA was extracted (explained above) and mixed with master mix of 5  $\mu$ L 10X Pfu turbo buffer, 1  $\mu$ L forward primer, 1  $\mu$ L reverse primer, 1  $\mu$ L 10mM dNTPs, 1  $\mu$ L Pfu turbo enzyme, and 10  $\mu$ L nuclease-free water. The mutagenesis reaction included 1  $\mu$ L of template DNA and 19  $\mu$ L master mix. The PCR cycles ran at 95°C for 1 minute; 18 cycles of 95°C for 50 seconds, 60°C for 50 seconds, 68°C for 1 minute/kb of plasmid



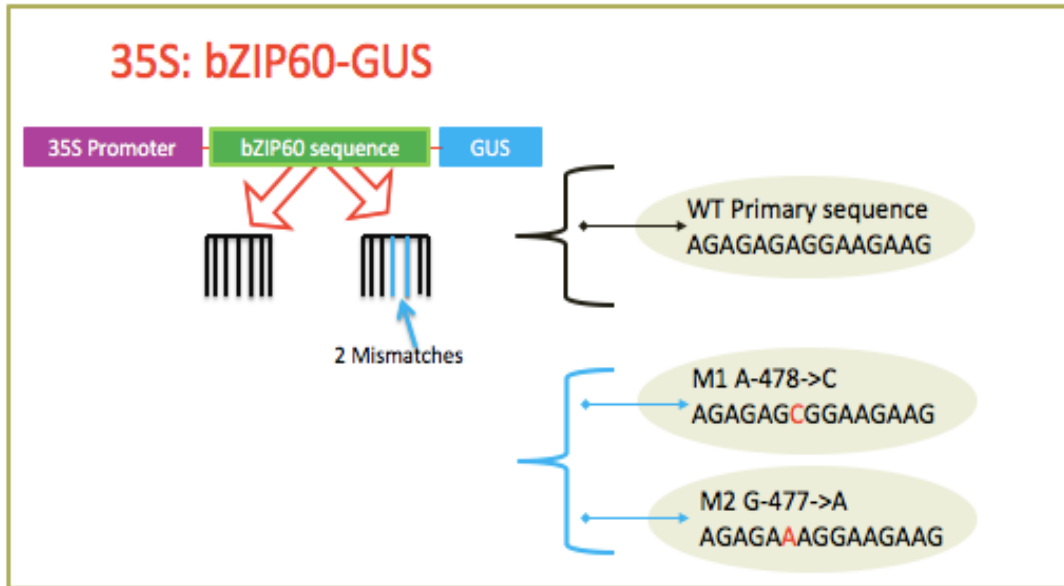
length, and 68°C for 7 minutes. 1 µL of Dpn1 was added to the reaction and incubated at 37°C for 1-2 hours.

### **Agrobacterium-mediated transformation**

Plasmids harboring 35S:bZIP60-GUS were transformed using *Agrobacterium tumefaciens* GV3101. 5-10 µL of plasmid sample (600 ng) and 50 µL of *Agrobacterium tumefaciens* GV3101 competent cell were mixed in an eppendorf tube and set on ice for 30 minutes. The tube is dropped into liquid nitrogen for 1 minute. The tube is then dropped into a 42°C water bath for 1 minute. Then, the tube is set back on ice for 2 minutes. 300 µL of YEB liquid media is added to the tube and set in a 200 rpm shaker at 28°C for 2 hours. The liquid is then streaked on YEB solid media supplemented with appropriate antibiotics and placed into 28°C incubator for 2 days.

### **Construction of miR5658-resistant versions of bZIP60 cDNA**

miR5658-resistant versions of bZIP60 cDNA were cloned and sequenced using the Sanger method explained above. Primers were developed with synonymous nucleotide substitutions introduced in their sequence for the miR5658-resistant versions of bZIP60 cDNA (Mutant1-A-478-C (M1) and Mutant2-G-477-A (M2)), as well as a primer for the non-mutated form of bZIP60 (WT) (Fig. 6).



**Figure 6. Mutagenesis Primer Design**

### **$\beta$ -glucuronidase (GUS) Assay**

*Agrobacterium tumefaciens* strain GV3101 harboring 35S:bZIP60-GUS were produced as described above. Four-week-old fingernail-sized *Arabidopsis* leaves were syringe infiltrated with *A. tumefaciens* GV3101 harboring a mutated form or non-mutated form of 35S:bZIP60-GUS into the abaxial surface. The plasmids that were introduced into the leaves are 35S:bZIP60-GUS (WT) (with a non-mutated binding sequence), and 35S:bZIP60-GUS (M1) and 35S:bZIP60-GUS (M2) (both with a mutated binding sequence at their respective positions) (Fig. 6). To test for GUS fluorescence a bacterial suspension of  $OD_{600} = 0.3$  containing 200  $\mu$ M acetosyringone was hand infiltrated into two leaves per plant and 12 plants/genotype per plasmid. Sampling in GUS required the removal of two leaves from the stem per plant three to five days post inoculation. Leaf samples were placed into a staining solution containing 830  $\mu$ L of water, 100  $\mu$ L of 0.1M  $NaPO_4$  pH 7.0, 20  $\mu$ L of 10mM EDTA, 10  $\mu$ L of 0.1% Triton X-100, 20  $\mu$ L of 1.0mM

$K_3Fe(CN)_6$ , and 20  $\mu$ L of 0.1M X-Gluc. Samples and solution was incubated for 2 days at 37°C. The staining solution was removed and replaced with 50% EtOH each following day. Pictures of leaves were taken using a camera and scanner.

### **$\beta$ -Galactosidase Assay (MUG) Assay**

Four-week-old fingernail-sized *Arabidopsis* leaves were infiltrated with *Agrobacterium tumefaciens* GV3101 harboring 35S:bZIP60-GUS (WT), 35S:bZIP60-GUS (M1) and 35S:bZIP60-GUS (M2) as explained above. Sampling in MUG required the removal of three leaves from the stem per genotype three to five days post inoculation. Samples were collected into liquid nitrogen and homogenized. 200  $\mu$ L of extraction buffer (50mM  $NaPO_4$  pH 7.0, 1mM  $Na_2EDTA$ , 0.1% SDS, 0.1% Triton X-100,  $H_2O$ , 1:500 Plant Protease Inhibitor Cocktail, and 10mM  $\beta$ -mercaptoethanol) was added to the samples and vortexed for 30 seconds. The samples were then centrifuged for 10 minutes at 4°C at 13 krpm. Samples were then added to the “assay plate” containing 190  $\mu$ L of assay buffer (extraction buffer + 11 mg MUG). Samples were taken out of the assay plate into the stop plate containing the stop buffer (0.2 Mm  $Na_2CO_3$ ) at time points 0hr, 1hr, 2hr and 3hr. Assay plate was kept in 4°C while the experiment took place.

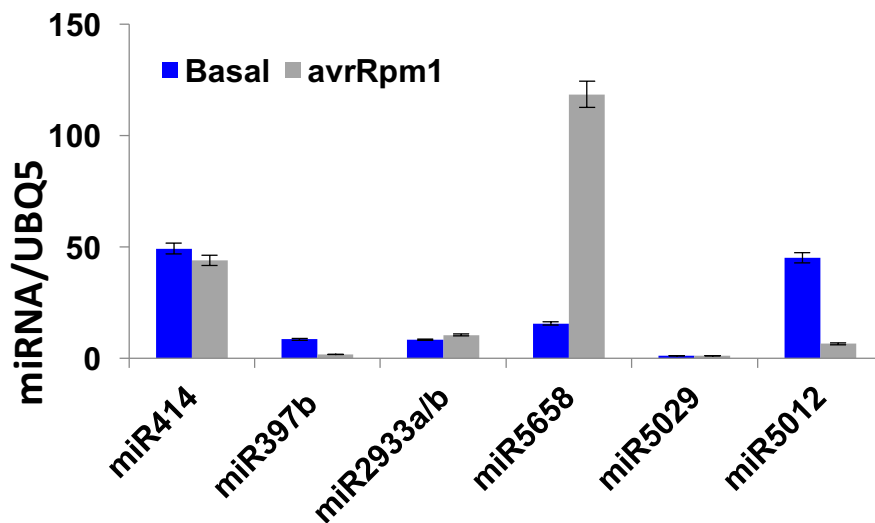
### **Agrobacterium-mediated plant transformation**

*Arabidopsis* plants are grown to flowering stage, and dipped twice with *Agrobacterium tumefaciens* GV3101 harboring 35S:bZIP60-GUS. Each genotype (*mel38*, *mel40*, *mel38/40*, *npr1*, Col-0) was dipped with each plasmid (35S:bZIP60-GUS (WT), 35S:bZIP60-GUS (M1) and 35S:bZIP60-GUS (M2)) to produce a comprehensive set of

lines, allowing to compare any differences between the genotypes and constructs. After dipping, the plants are allowed to grow normally to yield seeds to reveal any possible variation in seedling growth on specific media.

## RESULTS

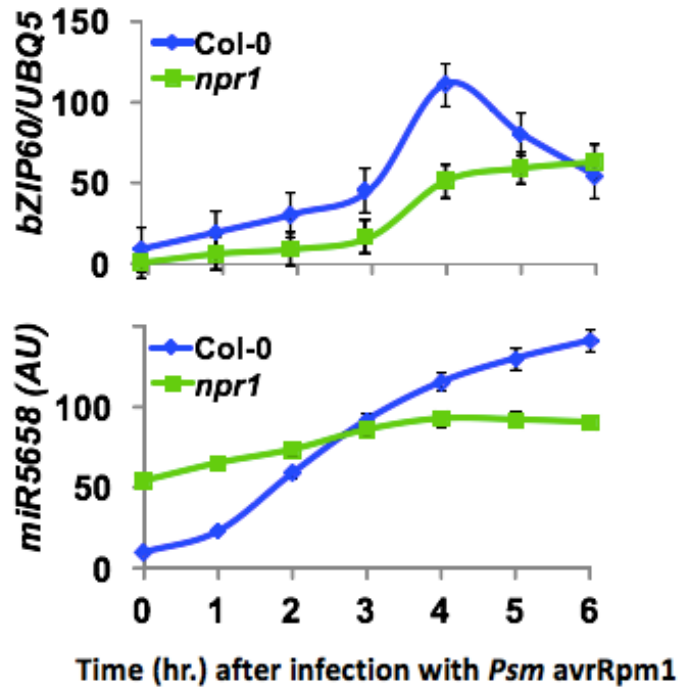
To investigate the role that the molecular IRE1a defense pathway plays in the plant cell, we first sought to understand the downstream effects of the pathway. Through preliminary research, we have found that miR5658 may be directly involved in the pathway because it is upregulated at times of biotic pathogen-induced stress (Fig. 7).



**Figure 7. miR5658 is upregulated during cell death induced by *Psm* ES4326 (*avrRpm1*).** Col-0 plants were infiltrated with *Psm* ES4326 (*avrRpm1*). Accumulation of several microRNA candidates shown to have binding specificity with bZIP60 was measured using quantitative real-time PCR (qRT-PCR).

Using an online miRNA binding prediction database “miRBase” it was discovered that bZIP60 mRNA might be targeted by six different miRNAs in Arabidopsis (Fig. 7). Wild-type (WT) Columbia (Col-0) plants were infiltrated with *Psm* ES4326 (*avrRpm1*) and miRNA transcript accumulation was measured using quantitative RT-PCR miRNA quantification assay. MiR5658 was determined to be the only candidate that displayed a marked upregulation compared to the other miRs tested. Through additional research, the

relationship between miR5658 and bZIP60 under biotic stress conditions was determined (Fig. 8). It was observed that upon bacterial infection, miR5658 expression increased, which coincided with a decrease in bZIP60 expression. The expression of bZIP60 in wild type (Col-0) and immuno-compromised *npr1* plants was determined to have a reciprocal relationship. Quantification of miR5658 revealed its induction coincides with bZIP60 mRNA suppression at 4 hrs post inoculation with avirulent bacteria. Also, upon transcript accumulation, we found that basal miR5658 expression was hyper-activated in *npr1* compared to Col-0. This suggested that miR5658 is in fact targeting bZIP60 mRNA for degradation during stressful conditions leading to the IRE1a pathway being forced towards the pro-death branch. Based on our preliminary data, we set forth to continue the proposed characterization of the IRE1a/miR5658 regulatory circuit to gain insights into molecular mechanisms of the cellular life/death switch.



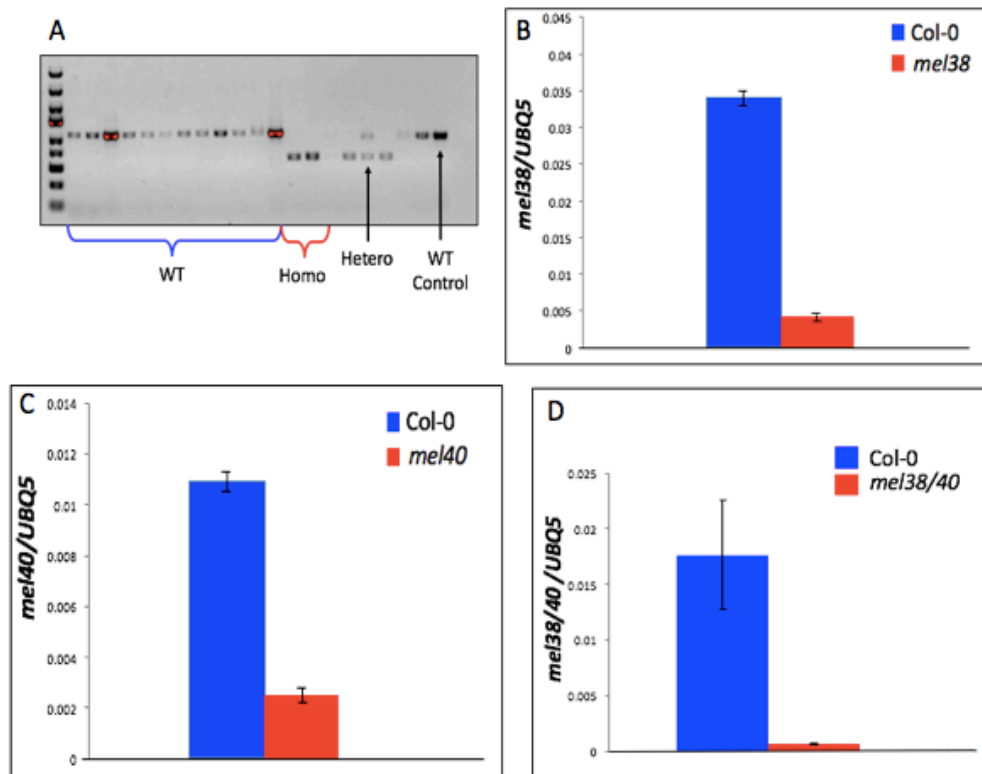
**Figure 8. Transcript accumulation of bZIP60 and miR5658.**

Col-0 and *npr1* plants were infiltrated with *Psm* ES4326 (*avrRpm1*). Accumulation of bZIP60 and miR5658 was measured using quantitative real-time PCR (qRT-PCR).

These preliminary results offered a path to continue our search for the key players involved in the plant defense pathways. Because bZIP60 mRNA is noted to be involved as a part of the pro-survival branch of the IRE1a-mediated defense pathway, we expect that miR5658 can participate in cellular transition into apoptosis through degradation of bZIP60 mRNA.

## Confirmation of homozygous miR5658 mutants

In order to validate our hypothesis that bZIP60 mRNA is targeted by miR5658, we first set out to obtain a set of genetic tools. We ordered seed of Arabidopsis lines with T-DNA insertions within At4g39838 and At4g39840, the two overlapping loci under investigation, from Arabidopsis Biological Resource Center at Ohio State University. I genotyped the plants to isolate miR5658 loss-of-function mutants (*mel38*, *mel40*, *mel38/40*) (see Materials and Methods), (Fig. 9).



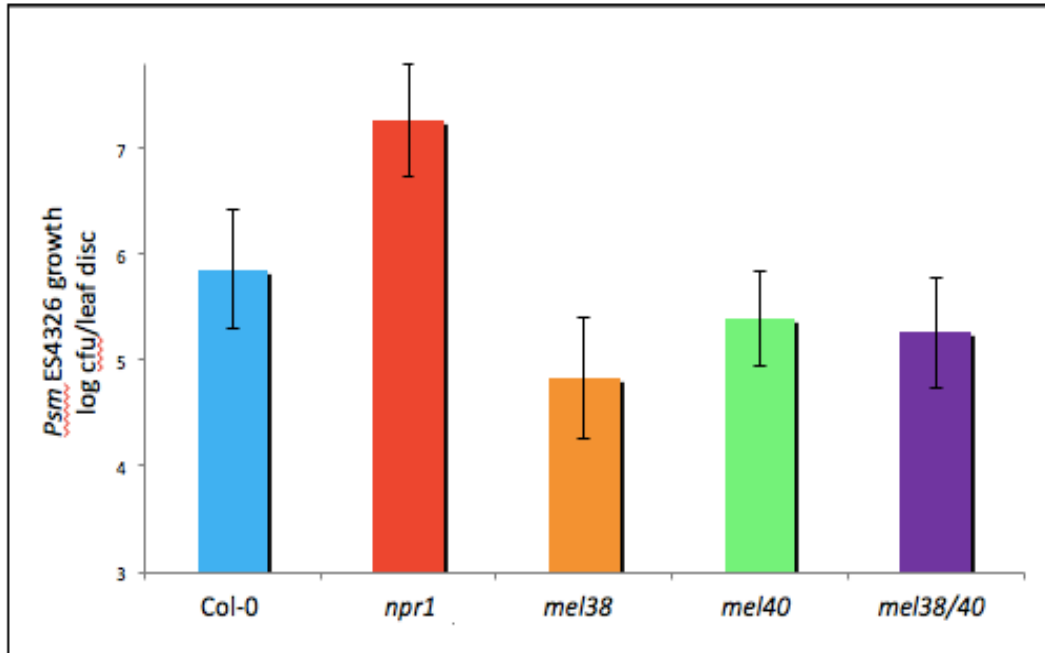
**Figure 9A-D. Homozygosity Analysis.** Homozygosity of individual plants were determined *via* gel electrophoresis and quantitative PCR (qPCR)-based protocol for genotyping plants. (A) PCR analysis using gene specific primer confirmed the homozygosity of all *mel* mutants. (B-D) Relative transcript levels of *MEL* was determined by qRT-PCR using cDNA generated from untreated 3-week-old WT, *mel38*, *mel40*, *mel38/40* plants. Error bars represent standard errors of three different technical replications. The experiment was performed three times with similar results.



Fig. 9A depicts a gel image from gel electrophoresis after genotyping PCR. It shows (i) a number of samples that have bands corresponding to the expected WT size, indicating homozygosity for the WT allele, (ii) four samples whose bands showing the sizes corresponding to T-DNA insertion within the gene, indicating homozygosity for the mutation, (iii) a pattern of two stacked bands depicting heterozygosity, and (iv) a positive control WT band included for reference and comparison purposes. Figure 9B-9D presents the results of qPCR-based quantification of three individual lines for miR5658: *mel38*, *mel40*, and *mel38/40*. Line named *mel38* has been disrupted in the At4g39838 locus, and *mel40* line has been disrupted in the At4g39840 locus. Both loci are disrupted in the *mel38/40* lines.

### **Bacterial Leaf Infiltration Assay- *Arabidopsis thaliana*-*Pseudomonas syringae* Pathosystem**

Having gained some insight into the IRE1a defense pathway, we sought to uncover the interconnection that is miR5658's role in the plant immune defense response upon bacterial infection infiltration with *Psm* ES4326. We intended to determine the specific disease phenotypes of our *mel* transgenic lines (*mel38*, *mel40*, *mel38/40*) lacking miR5658 compared to WT and immuno-compromised plants (Col-0 and *npr1* respectively).



**Figure 10. Bacterial log growth quantification of Wild-type (WT) Col-0 and mutant plants, *npr1*, *mel38*, *mel40*, and *mel38/40*.**




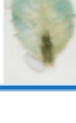
*Psm* ES4326 growth (colony forming units – cfu/leaf disc, expressed on a log scale) was quantified in four-week-old plants two days post syringe inoculation ( $OD_{600nm} = 0.001$ ). Error bars represent 95% confidence intervals of the mean ( $n = 4$ ). Experiments were repeated three independent biological replications with similar results. Analysis was conducted via quantification of bacterial growth on Kb-S media and converted to a graph for phenotypic comparison.

The data shown in Fig. 10 support our hypothesis that miR5658 is a key player in the plant defense immune pathway. Fig. 10 illustrates a representative outcome of an infection on the *mel* lines. As anticipated, we see reduced bacterial growth in *mel* plants compared to Col-0, which serves as the reference genotype. The immunocompromised genotype, *npr1*, lacking expression of *PR* genes exhibits the highest susceptibility compared to the others as expected. In fact, *npr1* bacterial growth is 1.5 log above than WT Col-0 growth levels. Mutant lines lacking miR5658: *mel38*, *mel40*, and *mel38/40*, are resistant to the pathogen compared to the Col-0 control and *npr1*, depicted by a lower level of pathogen growth. Pathogen growth in *mel38* displays 2 logs less than *npr1* and 1 log less than Col-0.

Pathogen growth in *mel40* and *mel38/40* displays 1.5 logs less than *npr1*, and 0.5 logs less than Col-0.

### **β-glucuronidase (GUS) Tissue Specific Expression Assay**

The Col-0 genotype possesses the ability to express miR5658, while *npr1*, *mel38*, *mel40*, and *mel38/40* transgenic genotypes are defective in the expression of miR5658 to various degrees. Plasmids 35S:bZIP60-GUS (WT), 35S:bZIP60-GUS (M1) and 35S:bZIP60-GUS (M2) were syringe infiltrated into each genotype. Initially, we decided to compare the differences between *mel* lines and Col-0 with the WT plasmid to experimentally test our hypotheses (Fig. 11).

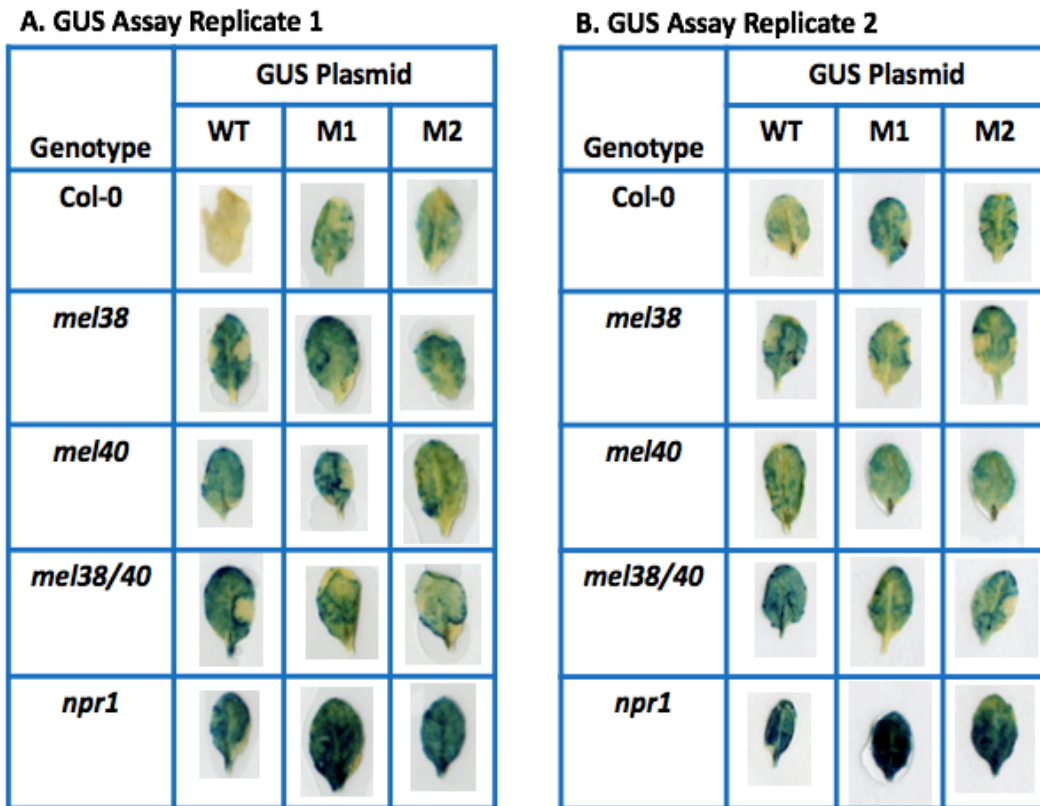
Genotype	GUS Plasmid
	WT
Col-0	
<i>mel38</i>	
<i>mel40</i>	
<i>mel38/40</i>	

**Figure 11. β-glucuronidase (GUS) assay results from WT plasmid.**

35S:bZIP60-GUS (WT) blue staining was quantified in four-week-old plants three days post syringe inoculation ( $OD_{600nm} = 0.5$ ). Experiments were repeated three independent biological replications with similar results. Analysis was conducted via a GUS stain with X-Gluc.

Staining was visible in the *mel* lines because miR5658 is absent so there should not be degradation of bZIP60 mRNA. Col-0 possesses the expression of miR5658, thus combined with the WT plasmid, miR5658-binding is permitted leading to degradation - exhibiting little or no blue staining.

Because our assumption proved accurate from our initial assay, we moved further to assess all genotypes with all plasmids (Fig. 12). We infiltrated replicates of Col-0, *npr1*, *mel38*, *mel40*, and *mel38/40* with *Agrobacterium tumefaciens* GV3101 harboring 35S:bZIP60-GUS (WT), 35S:bZIP60-GUS (M1), and 35S:bZIP60-GUS (M2).

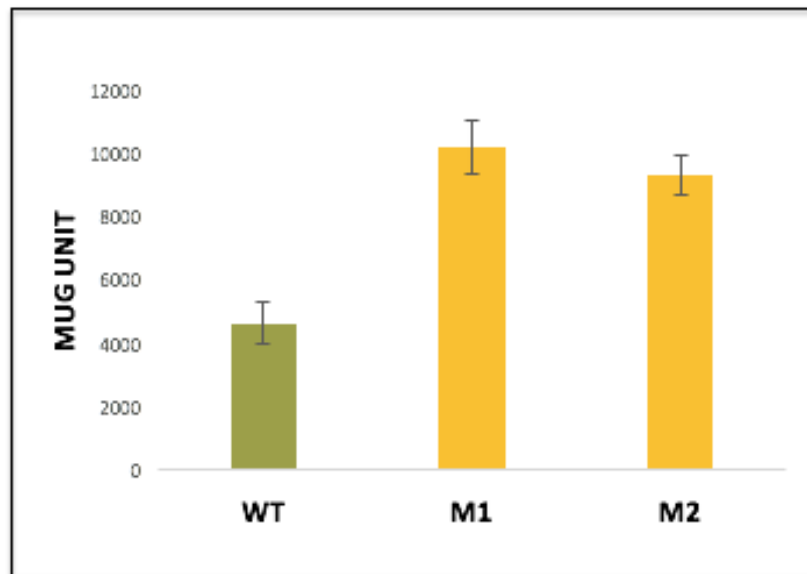


**Figure 12.  $\beta$ -glucuronidase (GUS) assay replicates.** 35S:bZIP60-GUS (WT), 35S:bZIP60-GUS (M1), and 35S:bZIP60-GUS (M2) blue staining was quantified in four-week-old plants three days post syringe inoculation ( $OD_{600nm} = 0.5$ ). Experiments were repeated four independent biological replications with similar results. Analysis was conducted via a GUS stain with X-Gluc.

As expected, blue staining was visible in all *mel* genotypes lacking functional miR5658. Also, as depicted above (Fig. 12), Col-0 plant sample with 35S:bZIP60-GUS (WT) plasmid results in little to no blue staining shown because miR5658 potentially degraded bZIP60. We also observed a difference in blue staining when compared to the two mutated plasmids, 35S:bZIP60-GUS (M1) and 35S:bZIP60-GUS (M2). When Col-0 is paired with a mutated plasmid blue staining is visible, therefore demonstrating that the abolished binding of miR5658 to bZIP60 potentially kept bZIP60 expression abundant. *npr1* plant samples provide important insight into the miR5658-regulated expression. The level of GUS blue staining in the *npr1* samples is significantly greater than all other genotypes tested.

## MUG Assay

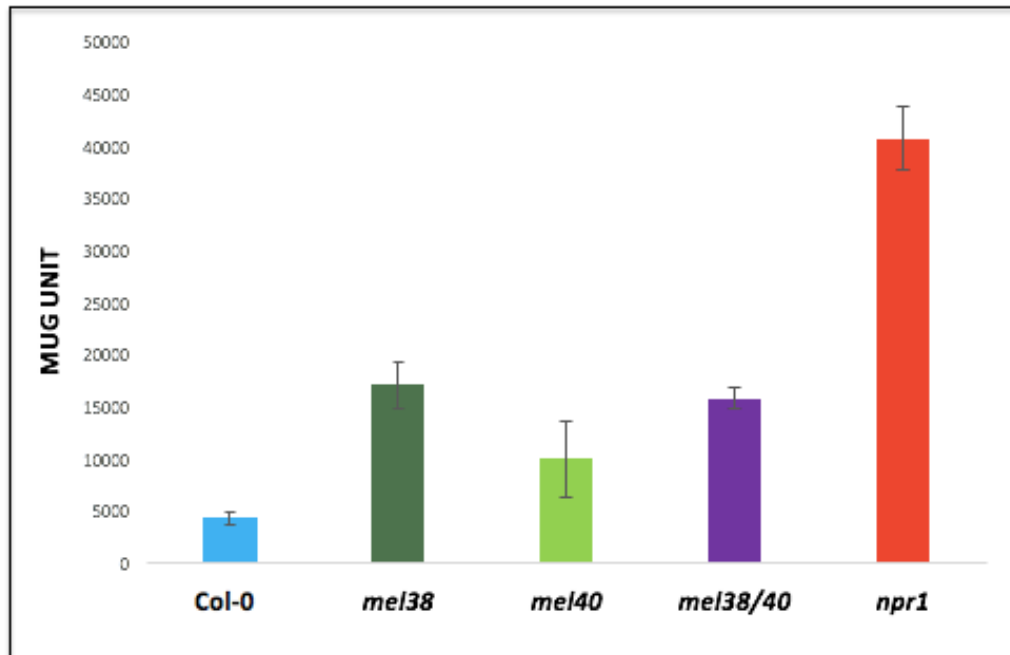
The MUG assay provided a measurable amount of bZIP60 accumulation in the plant leaf after infiltration with *Agrobacterium tumefaciens* GV3101 harboring 35S:bZIP60-GUS (WT), 35S:bZIP60-GUS (M1) and 35S:bZIP60-GUS (M2). We are able to obtain a measurable amount of bZIP60 fluorescence as it relates to miR5658 expression in MUG assay.



**Figure 13. 35S:bZIP60-GUS (WT), 35S:bZIP60-GUS (M1) and 35S:bZIP60-GUS (M2) infiltration MUG Assay of Col-0 plants.**

Four-week-old plants were syringe infiltrated with *Agrobacterium tumefaciens* GV3101 harboring 35S:bZIP60-GUS (WT), 35S:bZIP60-GUS (M1) and 35S:bZIP60-GUS (M2). bZIP60 accumulation was measured three days post syringe inoculation ( $OD_{600nm} = 0.5$ ). Experiments were repeated three independent biological replications with similar results.

The expression of bZIP60 was reduced after infiltration with *Agrobacterium tumefaciens* GV3101 harboring 35S:bZIP60-GUS (WT) compared to the mutated plasmids: 35S:bZIP60-GUS (M1) and 35S:bZIP60-GUS (M2). The mutated plasmids may abolish the binding of miR5658 to bZIP60 allowing the accumulation levels to rise.



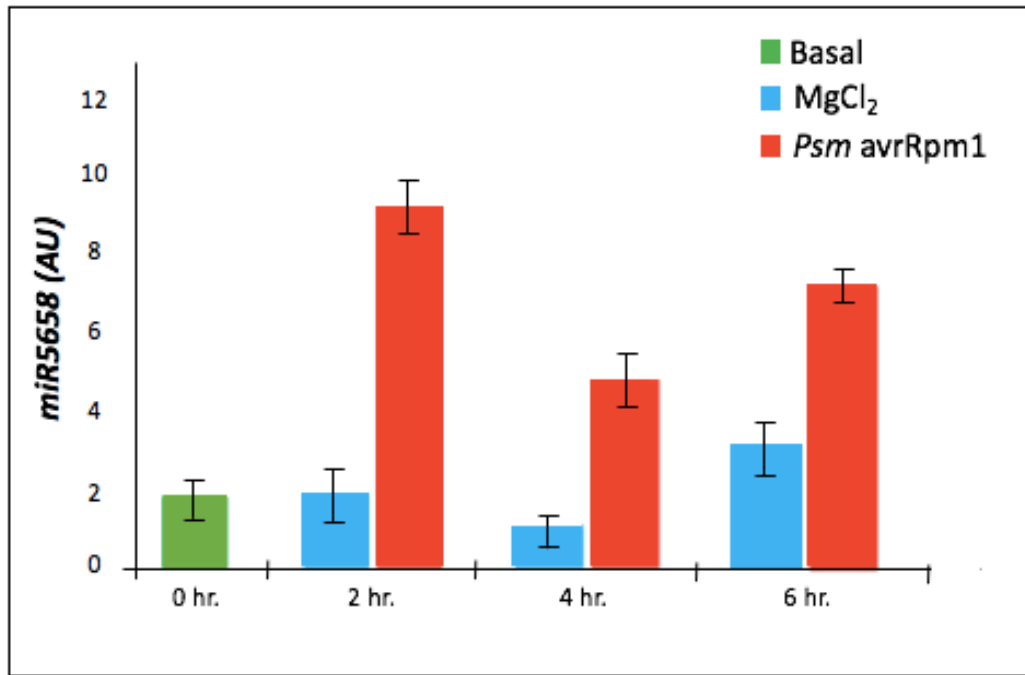
**Figure 14. 35S:bZIP60-GUS (WT) infiltration MUG Assay of Col-0, *npr1*, and *mel* lines.**

Four-week-old plants were syringe infiltrated with *Agrobacterium tumefaciens* GV3101 harboring 35S:bZIP60-GUS (WT). bZIP60 accumulation was measured three days post syringe inoculation ( $OD_{600nm} = 0.5$ ). Experiments were repeated three independent biological replications with similar results.

Wild-type bZIP60 accumulation levels was reduced compared to transgenic *mel* lines and *npr1* levels. All *mel* lines lacking miR5658 exhibit greater accumulation of bZIP60 compared to Col-0 which possesses miR5658. *npr1* mutant exhibits the greatest accumulation of bZIP60 in the leaf compared to all others because it may play a role in the regulation of miR5658.

### miR5658 Quantification Assay

We performed quantification of miR5658 in WT Col-0 and *npr1* plants under biotic stress conditions following infection with *Psm* ES4326. This provided insight into the expression of miR5658.



**Figure 15. Col-0 miR5658 quantification comparing pathogen stress to harmless MgCl<sub>2</sub>.** miR5658 basal expression is shown in green. miR5658 expression post *Psm* ES4326 challenge is shown in red. miR5658 expression post MgCl<sub>2</sub> infiltration is shown in blue. Error bars represent 95% confidence intervals of the mean (n = 6). Data represents two independent biological replications with similar results.

Col-0 plants were syringe infiltrated with *Psm* ES4326 or MgCl<sub>2</sub> to compare the expression levels of miR5658 at time points 0 hr (basal), 2 hr, 4 hr, and 6hr. The levels of miR5658 are markedly upregulated in response to pathogen stress as compared to MgCl<sub>2</sub> infiltration. The *Psm* ES4326 4 hr time point is lower when compared to time point 2 hr, however the expression levels start to increase again at time point 6 hr. A possible explanation of this fact is that this fluctuation is due to the circadian clock and diurnal gene regulation. The



expression levels measured in this experiment were the result of a combination of the circadian clock-driven expression and induction by a pathogen, and it is possible that at 4 hr the natural levels of this gene's expression were lower than at earlier and later time points.

Taken together, these results suggest that we may have identified a notable explanation for the role of the pro-survival to pro-death molecular switch in the IRE1a signaling pathway. Much is known about IRE1a signaling in yeast and mammals that has yet to be identified in plants. Initially, the structural analysis of the luminal domain of yeast IRE1 provided evidence into the activation of UPR. Past work suggests that the activation of the cytosolic domain of yeast IRE1 is instrumental to activating the endoribonuclease activity of IRE1 (Li H. et al., 2010). The mechanistic features of IRE1 activation are conserved in yeast, mammals, and consequently plants. In all eukaryotic systems tested so far IRE1 oligomerizes in the ER membrane and oligomerization correlates with the onset of IRE1 phosphorylation and RNase activity (Li H. et al., 2010). The activation of IRE1 can result in one of two pathways: pro-survival ER-stress relief signaling pathway or an apoptotic cell death, triggered upon acute or prolonged stress conditions. The mechanisms regulating cellular survival vs. cellular death during UPR are largely unknown in plants. Through this study, I attempt to provide evidence for the role of Arabidopsis IRE1a-splicing substrate, bZIP60, as the target for the molecular switch miR5658, which turns off the IRE1a-mediated pro-survival pathway. I also obtained genetic evidence that upon cell death-triggering stimuli, NPR1 may indirectly target and degrade bZIP60 mRNA *via* miR5658 to turn off the IRE1a-mediated pro-survival pathway.

## **FUTURE DIRECTION**

A GUS floral dip transformation is in the process for further investigation into bZIP60 tissue specific expression (See Materials and Methods). This procedure will produce stable Arabidopsis transgenics that express 35S:bZIP60-GUS (WT), 35S:bZIP60-GUS (M1) or 35S:bZIP60-GUS (M2), which offers a far more powerful tool than the leaves used in the previous work. Currently, we are awaiting T1 seeds and will initiate the analysis of transgenics shortly.

## DISCUSSION

The UPR is crucial to life as it regulates gene expression and homeostasis inside the cell in response to stress in the ER similarly amongst all eukaryotes (Zhang et al., 2015). All eukaryotes are equipped with the IRE1-mediated stress response pathway, but it remains largely unknown whether the downstream effectors are alike amongst the different kingdoms. Such mechanisms, if they were to exist and understood fully in the plant IRE1a/bZIP60 signaling, could form a foundation for further identification of important factors involved in agriculture and crop improvement. Our objective was to determine the specific activity of miR5658 on bZIP60 regulation *in planta* and use it to further our understanding of the IRE1 signaling pathway as a whole. We hypothesized that IRE1a-dependent bZIP60 splicing is a cytoprotective, adaptive mechanism, similar to the yeast and human IRE1/bZIP signaling that is involved in the pro-survival branch of the pathway. The hypothesis that bZIP60 can be regulated specifically by miR5658 is largely based upon homology between the miRNA and bZIP60 sequences. Furthermore, there is an analogous observation which has been made in the mammalian system, where the PERK pathway promotes miR-30c-2\* expression, which consequently suppresses XBP-1, a bZIP60 homolog, expression (Byrd et al., 2012).

Until now, a small fraction of conserved UPR pathways have been identified in eukaryotes. The first UPR sensor IRE1 was discovered in budding yeast as a type I transmembrane protein containing kinase and RNase activity. The most evolutionarily conserved UPR pathway is the IRE1-bZIP pathway, shown experimentally in humans and

yeast (Joshi et al., 2015). A detailed understanding of the many IRE1 activation mechanisms could potentially accelerate therapeutic development in humans (Joshi et al., 2015). Very recently, miRNA-controlled IRE1 regulation was discovered in mammals. This pathway, though not yet thoroughly understood in humans and yeast despite much foregoing research, bears the potential to be of great importance if elucidated in plants. Upon stress, the IRE1 enzymatic domains unconventionally splice the mRNAs of bZIP (basic leucine zipper) transcription factors *HAC1* (Homologous to Atf/Creb1), *bZIP60* and *XBP-1* (X-box binding protein 1) in yeast, plants, and mammals, respectively. This conservation of IRE1 throughout yeast, plants, and mammals drives our interest into understanding the regulation of bZIP60 mRNA in Arabidopsis. We propose that IRE1 signaling is attenuated by a specific miR5658 after prolonged ER stress. Past research explains that after attenuation, IRE1 enters a refractive state even if ER stress remains unmitigated (Li, H. et al., 2010). This attenuation includes dissolution of IRE1 clusters, IRE1 dephosphorylation, and decline in endoribonuclease activity; thus, IRE1 activity is believed to be governed by some sort of timer that could be important in “switching” the UPR from the pro-survival or cytoprotective phase to the pro-death or apoptotic phase (Li, H. et al., 2010).

MicroRNAs typically function in post-transcriptional regulation of gene expression; however, they were recently associated with the translation inhibition of secretory pathway proteins (Byrd et al., 2012). The analogous regulation of XBP-1 TF via miR-30c-2\* is a reputable indicator of the role that microRNAs can play as the molecular switch of particular secretory pathways. XBP-1 is a key TF that is involved in the pro-survival branch of the PERK pathway, which is reminiscent of the IRE1a-bZIP60 TF also

involved in cellular survival of the UPR pathway. Byrd et al. (2012) supplied the initial connection between a microRNA and the direct regulation of the ER stress response, and provided us with the novel molecular regulation of XBP-1 via miR-30c-2\* to use as a means for our own research. Byrd et al. (2012) showed miR-30c-2\* expression increases in response to tunicamycin treatment, in which is remarkably in agreement with our study, showing that miR5658 expression increased in response to another ER stress signal, the pathogen *Psm* ES4326 infection. There is a noted fluctuation of miR-30c-2\* expression observed and is deduced to the circadian clock of the plant (Byrd et al., 2012). This conclusion helped to give merit to our rationale that the fluctuation of miR5658 seen after pathogen infection (Fig. 13) is attributed to the normal circadian rhythm of the plant, and is further substantiated by analyses of circadian expression of the locus under study in the Plant Diurnal Expression Database (<http://diurnal.mocklerlab.org/>).

Through stress-related assays, we showed that the absence of miR5658 expression results in resistance to bacterial disease in *mel* plants compared to WT Col-0 plants (Fig 10). The microRNA, miR-30c-2\*, was experimentally shown to negatively regulate XBP-1 TF via degradation of XBP-1 mRNA (Byrd et al., 2012). The negative regulation of XBP-1 in an analogous system provides justification for our proposal that miR5658 is a negative regulator of the IRE1a pathway via degradation of bZIP60 mRNA. Along these lines, we believe that miR5658 is involved in the immune response serving as a molecular switch transitioning the cell into apoptosis upon pathogen attack. Our explanation of this result is that in the absence of miR5658, the cell fails to degrade bZIP60, whose stress-adaptive functions help to cope with the infection. We have proposed that, upon lethal levels of stress, miR5658 will target and bind to bZIP60 mRNA to initiate mRNA decay of this pro-

survival factor. This perspective is experimentally shown in the *mel* lines lacking miR5658, because the absence of miR5658 contributes directly to disease resistance (Fig. 10). Together these results help to verify our initial rational that miR5658 is involved in the immune response of the plant.

We also suggested that NPR1 will regulate the following processes: (i) down-regulation of bZIP60 transcript through the regulation of miR5658 expression and (ii) activation of the pro-apoptotic branch of the IRE1a signaling pathway. The detection of disturbance or stress in the ER leads to the activation of IRE1-mediated signaling pathway, transducing the stress signal from ER to nucleus - where we propose NPR1 may play a part by regulating miR5658. The nuclear factor-kappa B (NF- $\kappa$ B) is the functional equivalent of NPR1 in that it too operates in prompt posttranscriptional regulation in response to stress signals (Baeuerle and Henkel, 1994). The mammalian PERK pathway, mentioned above, provides experimental evidence to associate the functionality of NF- $\kappa$ B to NPR1, by virtue of how NF- $\kappa$ B is activated upon stress signals (Byrd et al., 2012). Similar to NF- $\kappa$ B, NPR1 is activated upon recognition of stress and the stimulation of homeostatic restoration in the cell (Kinkema et al., 2000). NF- $\kappa$ B is a family of proteins that regulate a multitude of genes involved in stress responses including inflammation and apoptotic cellular suicide (Karin et al., 2002) (Li and Verma, 2002). The PERK pathway frees NF- $\kappa$ B in the cytoplasm for transfer to the nucleus where it activates target genes or ER stress genes. Bioinformatics analysis of the sequence of NF- $\kappa$ B exhibited the potential binding site relationship between NF- $\kappa$ B and miR-30c-2\* (Byrd et al., 2012). The discovery of NF- $\kappa$ B's relationship with miR-30c-2\* provided a basis to relate master regulatory proteins with specific microRNAs within the immune response. In our model, we propose that NPR1, along with some TF,

regulates the expression of miR5658 in response to prolonged stress. We have presented evidence that NPR1 in *Arabidopsis* functions in part within the immune response considering mutants are defective in resistance to infections (Figs. 10 and S3). Furthermore, additional studies demonstrate that *npr1* mutant plants fail to respond to various SAR-inducing treatments, displaying little expression of PR genes as well as exhibiting increased susceptibility to disease (Cao et al., 1997).

microRNAs have been acknowledged as a central player in controlling cellular fate since their discovery in 1993 (Wang 2010). These short nucleotide molecules can act as repressors of proapoptotic or antiapoptotic genes, earning their spot as potential novel therapeutic targets for the treatment of disease (Wang 2010). Through the initial understanding of the conserved role for microRNA regulation of the plant innate immune system, we want to assimilate the molecular mechanism governing the “switch” from life to death. We examine the cleavage of a pro-survival factor via nta-miR6019 or nta-miR6020 as the molecular switch from life to death, as proposed in our model with miR5658. MicroRNAs will incorporate themselves into the RISC by binding to a small region of the 3'UTR. The important component of microRNA-RISC binding is the extra single stranded nucleotides in the microRNA sequence are free to bind to mRNAs in the cytoplasm. The complementarity with the rest of the sequence of a miRNA plays the crucial role in PTGS gene regulation, aka the molecular switch in life or death of the cell. The functionality of the mRNA targeted by the microRNA-RISC is critical in “choosing” the outcome, however because the microRNA is the molecular factor that specifically binds and degrades the proapoptotic or antiapoptotic mRNA, it should be known as the molecular switch.

We propose miR5658 will target bZIP60 mRNA for decay through binding with the RISC and bZIP60 mRNA. It is generally acknowledged that microRNAs recruit the RISC for degradation of mRNA, however we sought to experimentally show that miR5658 does bind specifically to miR5658 for decay. The  $\beta$ -glucuronidase (GUS) assay is advantageous molecular biology technique because its presents a visualized expression of miR5658 regulation on bZIP60 *in planta*. In our study, we wanted to determine the tissue specific expression through GUS staining of the transgenics and WT plants. The Arabidopsis IRE1 signaling pathway mediates sequence-specific bZIP60 splicing and can promiscuously degrade ER-bound mRNAs via RIDD (regulated IRE1-dependent decay of mRNA). We hypothesized that, under prolonged ER stress, the IRE1a-bZIP60 signaling needs to be attenuated via miR5658 binding to bZIP60 mRNA. Therefore, there must be a portion of the bZIP60 sequence that perfectly, or imperfectly, can bind to miR5658. This logic is what led us to believe that by mutating the binding portion of the sequence would lead to the inhibition of miR5658 binding, and therefore an inhibition of the degradation process. In collaboration with a visiting post-doctoral scholar in the lab (Dr. Ahmed Amer), miR5658-resistant versions of bZIP60 cDNA were engineered manually through analyzing the miR-binding region of bZIP60 mRNA and mutagenizing the predicted miR5658 binding site. This approach allows us to abolish the binding of miR5658, while not altering the encoded amino acid sequence. Thereupon, Arabidopsis leaves were syringe infiltrated with *Agrobacterium tumefaciens* GV3101 harboring 35S:bZIP60-GUS (WT), 35S:bZIP60-GUS (M1), 35S:bZIP60-GUS (M2) to determine the differences between Col-0 leaves possessing miR5658, *mel* transgenic lines lacking miR5658, and *npr1*



hypothesized to have heightened expression of miR5658. MicroRNAs can bind to complementary sequences within the 3'-untranslated regions (3'-UTR) of their target mRNAs to induce degradation through the RISC (Wang et al., 2008). In the mammalian mouse model, over 30 microRNAs were observed that can directly bind to TF's with complementary sequences (Wang et al., 2008). From our model, we corroborate that our miR5658 in fact also does bind to a TF, bZIP60, to initiate mRNA decay through RISC (Figs. 11 & 12).

Posttranscriptional gene silencing (PTGS) is involved in the regulation of host defense against pathogenic attack (Li et al., 2012). PTGS is a RNA degradation system that is most notably known in plants and analogous to RNA interference in animals (Vaucheret et al., 2001). We lack a complete understanding of the mechanism; however, some microRNAs involved in the regulation of the plant innate immune system have been recorded. Recently, two specific microRNAs, nta-miR6019 and nta-miR6020, were documented to have a direct involvement in the PTGS of *Nicotiana benthamiana* (Li et al., 2012). *Nicotiana benthamiana* is a valuable heterologous host plant for transient assays of *Arabidopsis thaliana*. Therefore, the recognition of two specific microRNAs involved in the innate immune system of *Nicotiana benthamiana* is of great interest for our study of *Arabidopsis*. nta-miR6019 and nta-miR6020 guide sequence-specific cleavage of transcripts of the nucleotide binding-leucine-rich repeat immune receptor N that confers resistance to tobacco mosaic virus. This mechanism is similar to miR5658 sequence-specific cleavage of bZIP60 mRNA which is directly involved in the transcription of ER stress genes.

The elucidation of the pro-survival to pro-death molecular switch is crucial because the plant world is at risk. Together our results help to verify our initial rationale that miR5658 is involved in the immune response of the plant. Specifically, we propose that miR5658 is functioning as a molecular switch to degrade a key pro-survival downstream player in the IRE1a pathway, bZIP60 mRNA. IRE1 is conserved amongst eukaryotes as a major UPR sensor. Therefore, the understanding of the IRE1/bZIP60 signaling in the plant kingdom could prove to be useful for further investigation amongst all eukaryotes. There is also a need for the understanding of the regulation of miR5658 because of the role it plays in the pro-death branch of the IRE1a pathway. Based on our findings, we hypothesize that NPR1 together with an unknown transcription factor may be a direct regulator of miR5658 expression. These conclusions provide us with a foundation of the understanding of the elusive IRE1a signaling pathway in *Arabidopsis thaliana*.

## LIST OF REFERENCES

- Anand, A., Uppalapati, S. R., Ryu, C., Allen, S. A., Kang, L., Tang, Y., Mysore, K. S.  
Salicylic Acid and Systemic Acquired Resistance Play a Role in Attenuating  
Crown Gall Disease Caused by *Agrobacterium tumefaciens*. *Plant Physiology*.  
146(2): 703-715. Feb 2008.
- Baeuerle P.A. and Henkel T. Function and Activation of Nf-kappaB in the Immune  
System. *Annual Review of Immunology*. 12:141-179. 1994.
- Boatwright, J.L. Regulatory Mechanisms of Pathogen-mediated cellular stress  
signaling in *Arabidopsis thaliana*. Master's Thesis. Birmingham, AL. 2013.
- Bigeard, J., Colcombet, J., Hirt, H. Signaling Mechanisms in Pattern-Triggered  
Immunity (PTI). *Molecular Plant*. Vol. 8. Issue 4. (521-539) Apr 2015.
- Byrd AE, Aragon IV, Brewer JW. MicroRNA-30c-2\* limits expression of  
proadaptive factor XBP1 in the unfolded protein response. *J Cell Biol*, vol.  
196, pp. 689-698, 2012.
- Cao H., Glazebrook J., Clarke J.D., Volko S., Dong X. The *Arabidopsis* NPR1 gene  
that controls systemic acquired resistance encodes a novel protein containing  
Ankyrin repeats. *Cell*. 1997 Jan 10; 88(1):57-63.
- Dalmay, Tamas. Mechanism of MiRNA-mediated Repression of MRNA Translation.  
*Essays In Biochemistry*. (54): 29-38. 2013.
- Dodds, P. N. and Rathjen, J. P. Plant immunity: towards an integrated view of plant –  
pathogen interactions. *Nature Reviews*. 11, 539-548. Aug 2010.

- Fanata, D., SY, L., KO, L., The unfolded protein response in plants: a fundamental adaptive cellular response to internal and external stresses. *J Proteomics*. 93: 356-68. Nov 2013.
- Guillemette, T., Iacomi-Vasilescu, B. and Simoneau, P. (2004) Conventional and real-time PCR-based assay for detecting pathogenic *Alternaria brassicae* in cruciferous seed. *Plant Dis*, **88**, 490-496.
- Hetz, Claudio. The Unfolded Protein Response: Controlling Cell Fate Decisions under ER Stress and beyond. *Nature Reviews Molecular Cell Biology Nat Rev Mol Cell Biol* (2012): 89-102.
- Jones, J. D. G. and Dangl, J. L. The plant immune system. *Nature*. 444, 323-329. Nov 2006.
- Joshi, A., et al. Molecular mechanisms of human IRE1 activation through dimerization and ligand binding. *Oncotarget*, 2015. 6(15): p. 13019-13035.
- Karin M., Cao Y., Greten F.R., Li Z.W. NF-kappaB in cancer: from innocent bystander to major culprit. *Nature Reviews Cancer*. 2002 Apr 2(4):301-10.
- Kinkema, M., Fan W., Dong X. Nuclear Localization of NPR is Required for Activation of PR Gene Expression. *Plant Cell*. 2000 Dec 12(12): 2339-2350.
- Li F., Pignatta D., Bendix C., Brunkard J., Cohn M., Tung J., Sun H., Kumar P., Baker., MicroRNA regulation of the plant innate immune receptors. *Proceedings of the National Academy of Science USA*. 2012 Jan; 109(5): 1790-1795.

- Li H., Korennykh A. V., Behrman S. L., Walter, P. Mammalian endoplasmic reticulum stress sensor IRE1 signals by dynamic clustering. *CrossMark*. 107(37) 16113-16118. 2010.
- Li Q. and Verman I.M. NF-kappaB regulation in the immune system. *Nature Reviews Immunology*. 2002 Oct 2(10): 725-34.
- Liu, Xiaoyu, Yali Sun, Camilla J. Kørner, Xinran Du, **Marie E. Vollmer**, and Karolina M. Pajerowska-Mukhtar. Bacterial Leaf Infiltration Assay for Fine Characterization of Plant Defense Responses Using the *Arabidopsis Thaliana-Pseudomonas Syringae* Pathosystem. *Journal of Visualized Experiments JoVE* (104) 2015.
- Moreno, A.A., et al. IRE1/bZIP60-Mediated Unfolded Protein Response Plays Distinct Roles in Plant Immunity and Abiotic Stress Responses. *PLoS One*, 2012. 7(2): p. e31944.
- Nagashima, Yukihiro, Kei-Ichiro Mishiba, Eiji Suzuki, Yukihiro Shimada, Yuji Iwata, and Nozomu Koizumi. Arabidopsis IRE1 catalyses unconventional splicing of bZIP60 mRNA to produce the active transcription factor. *Scientific Reports*, 2011. 1(29): p. srep00029.
- Nilsen, Erik T., David M. Orcutt, and Maynard G. Hale. *The Physiology of Plants under Stress*. New York: Wiley, 1996.
- Nimchuk, Z., Eulgem, T., Holt III, B. F., Dangl, J. L. Recognition and Response in the Plant Immune System. *Annual Review of Genetics*. 37: 579-609. Dec 2003.

- Osowski, Christine M., and Fumihiko Urano. Measuring ER Stress and the Unfolded Protein Response Using Mammalian Tissue Culture System. *The Unfolded Protein Response and Cellular Stress, Part B Methods in Enzymology* 2011 (490): 71-92.
- Population, Total. *World Bank*. The World Bank Group, Web.
- Serine/threonine-protein Kinase/endoribonuclease IRE1a." IRE1A. UniProt.
- Sotiropoulou, Georgia., Pampalakis, Georgios, Lianidou, and Mourelatos, Zissimos. Emerging roles of microRNAs as molecular switches in the intergrated circuit of the cancer cell. *RNA*. 2009 Aug; 15(8): 1443-1461.
- Srivastava, R., Y. Deng, S. Shah, A. G. Rao, and S. H. Howell. BINDING PROTEIN Is a Master Regulator of the Endoplasmic Reticulum Stress Sensor/Transducer BZIP28 in Arabidopsis. *The Plant Cell* 25.4 (2013): 1416-429.
- Sunkar, Ramanjulu, and Jian-Kang Zhu. Novel and Stress-Regulated MicroRNAs and Other Small RNAs from Arabidopsis. *The Plant Cell Online*. 2004.16(8): 2001-019.
- Taylor, Leslie. *The Healing Power of Rainforest Herbs: A Guide to Understanding and Using Herbal Medicinals*. Garden City Park, NY: Square One, 2005.
- Tsuda, K. and Katagiri, F. Comparing signaling mechanisms engaged in pattern-triggered and effector-triggered immunity. *Current Opinion in Plant Biology*. 13(4): 459-465. Aug 2010.
- Vaucheret H., Beclin C., Fagard M. Post-transcriptional gene silencing in plants. *Journal of Cell Science*. 114, 3083-3091. 2011.

Wang G., Wang X., Wang Y., Yang J., Nephew K., Edenburg H., Zhou F., Liu Y.

Identification of transcription factor and microRNA binding sites in  
responsible to fetal alcohol syndrome. *BMC Genomics*. 2008 Mar 20.

Wang Z., MicroRNA: A matter of life or death. *World Journal of Biological  
Chemistry*. 2010 Apr; 1(4): 41-54.

Wu, Yue, Di Zhang, Jee Yan Chu, Patrick Boyle, Yong Wang, Ian D. Brindle,  
Vincenzo De Luca, and Charles Després. The Arabidopsis NPR1 Protein Is a  
Receptor for the Plant Defense Hormone Salicylic Acid. *Cell Reports*.  
2012;1(6): 639-47.

Zhang, Baohong, Xiaoping Pan, George P. Cobb, and Todd A. Anderson. Plant  
MicroRNA: A Small Regulatory Molecule with Big Impact. *Developmental  
Biology* 289.1 (2006): 3-16.

Zhang L, Chen H, Brandizzi F, Verchot J, Wang A (2015) The UPR Branch IRE1-  
*bZIP60* in Plants Plays an Essential Role in Viral Infection and Is  
Complementary to the Only UPR Pathway in Yeast. *PLoS Genetics* 2015  
11(4): e1005164. doi:10.1371/journal.pgen.1005164

## APPENDIX A

### *Supplemental material*

MV 1	ggggacaagtttgatacaaaaaagcaggctccAT GTCTCCACTCAAGTACTTGTGT	F cDNA At4g39840 gene cloning
MV 2	ggggaccactttgtacaagaaagctgggtcTCA ATTTTTCTTCCCTTCGTCACC	Rstop cDNA At4g39840
MV 3	ggggaccactttgtacaagaaagctgggtcATT TTTCTTCCCTTCGTCACCGCC	Rstopless cDNA At4g39840
MV 4	ggggacaagtttgatacaaaaaagcaggctccG AGTCAAAGTCGTTGATCGTTGACTT GG	F promoter cloning 40
MV 5	ggggaccactttgtacaagaaagctgggtcGGC AAAGAAAGAAGAAGAAGAGAATAG	R promoter cloning 40
MV 6	TCTGCATTATTACGTGGCGG	qRT PCR specific to 40 F
MV 7	CCGTGTATCTCCAGTTCGTC	qRT PCR specific to 40 R
MV 8	ggggacaagtttgatacaaaaaagcaggctccG AGGTACATGAGAAGAAGCAAGAG	F cDNA At4g39838 gene cloning
MV 9	ggggaccactttgtacaagaaagctgggtcACT ACTACTCACGTACAATGAAAC	R cDNA At4g39838 gene cloning
MV 10	ggggacaagtttgatacaaaaaagcaggctccAA GTTAAAAGTCAATACTTTTCACAAA	F promoter cloning 38
MV 11	ggggaccactttgtacaagaaagctgggtcCTC TACGCAACATCGAGCTCAACATACG	R promoter cloning 38
MV 12	TAACCGCACCGTCATGTTGC	AT4G39838/qRT- PCR/Forward#1
MV 13	CCGCACCGTCATGTTGCAGA	AT4G39838/qRT- PCR/Forward#2
MV 14	ACTACTACTCACGTACAATG	AT4G39838/qRT- PCR/Reverse#1
MV 15	CTACTCACGTACAATGAAAC	AT4G39838/qRT- PCR/Reverse#2
MV 16	TCTGTCCAAATCAAGCTCATCC	Common/qRT- PCR/Forward
MV 17	TTCTCTGATGGAGGTGAAGAAAG	Common/qRT- PCR/Reverse
MV 18	GCAGATCTGTCCAAATCAAGC	LP #5/ At4g39840 homo #093172
MV 19	AAAAGTTTCCAACCATCCACC	RP #5/At4g39840 homo #093172



MV 20	AAGTGTCGTTTTGGTCCTCC	LP #6/At4g39838 homo #047112
MV 21	TAGGAGGAGGAGGAAGATTGG	RP #6/At4g39838 homo #047112
MV 22	TGAGAAATGAGTGGCCCATAC	LP #4/ At4g39840 homo #074898
MV 23	CACCAACCATAGCTTCCGTAG	RP #4/ At4g39840 homo #074898
MV 24	CTACGGAAGCTATGGTTGGTG	LP #3/ 38/40 #028622
MV 25	AGAGAATCTGCAACATGACGG	RP #3/ 38/40 #028622
MV 26	CTCTACGATTCCGTAGACCCC	LP #1/ At4g39840 homo #097507
MV 27	CATTCTGGCTAGACGACGAAG	RP #1/ At4g39840 homo #097507
MV 28	CTCTACGATTCCGTAGACCCC	LP #2/ 38/40 #104462
MV 29	CATTCTGGCTAGACGACGAAG	RP #2/ 38/40 #104462
MV 30	ATCCCTAATCCCAGACCTAGAG	38/40 Forward middle sequence
MV 31	GAAAGAGACTACGGAAGCTATGG	38/40 Reverse middle sequence
MV 32	CTTTGTGGGCTTTGCTGTAG	40 forward end sequence qPCR
MV 33	CCGTGTATCTCCAGTTCGTC	40 reverse end sequence qPCR
MV 34	GCCAACAAACAGATCACCAA	#4 RP
MV 35	TTTTTCTTCCCTTCGTCACC	#4 RP
MV 36	AACCACAATCCGTGGAGAAG	#2 LP
MV 37	AAAACCCCAAGTTCCAAAC	#2 RP
MV 38	GAAGCTCAATTCCGGAACAA	#1 LP
MV 39	CTGACGAAGCACCACCCTAT	#1 RP
MV 40	ggggaccactttgtacaagaaagctgggtcGTT CACGGGTCTTTAAACTGG	P38 F Internal N251
MV 41	ggggaccactttgtacaagaaagctgggtcCGC CAATCCACCGACACAAG	P38 F Internal N750
MV 42	ggggaccactttgtacaagaaagctgggtcCGG GCCATGTGAGTATCTCC	P40 F Internal N289
MV 43	ggggaccactttgtacaagaaagctgggtcCAG AAGTGACAAATACCATT	P40 F Internal N782
MV 44	ggggaccactttgtacaagaaagctgggtcGA GGGACGAGGATGAAGACG	G38 F Internal N240
MV 45	ggggaccactttgtacaagaaagctgggtcTGG TGGTGGTCTTGGCGAGT	G38 F Internal N744

MV 46	ggggaccactttgtacaagaaagctgggtcCAT CATCATCATCTGGTACT	G40RS & RSL F Internal N251
MV 47	ggggaccactttgtacaagaaagctgggtcCAA AGCCAACAAACAGATCACC	G40RS & RSL F Internal N756
MV48	AGAGAGAGGAAGAAG	mir5658 regular F
MV49	CTTCTTCCTCTCTCT	mir5658 reg R
MV50	CGAGAAAGGAAGAAG	mir5658 1,3 F changes
MV51	CTTCTTCCTTTCTCG	mir5658 1,3 R
MV52	AGGGAGCGGAAGAAG	mir5658 2,4 F
MV53	CTTCTTCGCTCCCT	mir5658 2,4 R
MV54	AGAGAAAGGAAAAAG	mir5658 3,6 F
MV55	CTTTTTCTTTCTCT	mir5658 3,6 R
MV56	AGAGAACGCAAGAAG	mir5658 3,4,5 F
MV57	CTTCTTGCGTTCTCT	mir5658 3,4,5 R
MV58	AGGGAGAGGAAGAAG	2 CHANGE F
MV59	CTTCTTCCTCTCCCT	2 CHANGE R
MV60	AGAGAAAGGAAGAAG	3 CHANGE F
MV61	CTTCTTCCTTTCTCT	3 CHANGE R
MV62	AGAGAGCGGAAGAAG	4 CHANGE F
MV63	CTTCTTCGCTCTCT	4 CHANGE R
MV64	AGAGAGAGGAAAAAG	6 CHANGE F
MV65	CTTTTTCTCTCTCT	6 CHANGE R
MV66	AGAGAGAGAAAGAAG	5 CHANGE F
MV67	CTTCTTTCTCTCTCT	5 CHANGE R
MV68	GCGGTTAGATCGAGGGAGCGG AAGAAGGAATAT	DOUBLE 2,4
MV69	ATATTCCTTCTTCCGCTCCCTCGATCTA ACCGC	D 2,4 RC
MV70	AGATCGAGAGAGCGGAAAAAG GAATATGTA	DOUBLE 4,6
MV71	TACATATTCCTTTTTCCGCTCTCTCGAT CT	D 4,6 RC
MV72	GCGGTTAGATCGCGAGAAAGG AAGAAGGAA	DOUBLE 1,3
MV73	TTCCTTCTTCTTTCTCGGATCTAACC GC	D 1,3 RC
MV74	GCGGTTAGATCGCGAGAGAGG AAGAAG	SINGLE 1
MV75	CTTCTTCCTCTCTCGGATCTAACCGC	S 1 RC

MV76	GTTAGATCGAGAGAAAGGAAG AAGGAA	SINGLE 3
MV77	TTCCTTCTTCCTTTCTCTCGATCTAAC	S 3 RC
MV78	GTTAGATCGAGAGAACGCAAGA AGGAATAT	TRIPLE 3,4,5
MV79	ATATTCCTTCTTTCGTTCTCTCGATCTA AC	T 345 RC
MV80	GCGGCGGTTAGATCGAGAGAAAGGA AGAAGGAATATGTAC	SINGLE 3 F
MV81	GTACATATTCCTTCTTCCTTTCTCTCGA TCTAACCGCCGC	SINGLE 3 RC
MV82	GCGGTTAGATCGAGAGAGCGGAAGA AGGAATATGTACAAG	SINGLE 4 F
MV83	CTTGTACATATTCCTTCTTCGCTCTCT CGATCTAACCGC	SINGLE 4 RC

**Table S1. Primers.**

gene cloning primers
promoter cloning primers
qRT-PCR primers
SALK TDNA primers
New SALK TDNA primers
mir5658/bzip60 primers
mir5658/bzip60 primers with GC content and >25bps
CORRECT MIR BZIP PRIMERS for mutagenesis

**Table S2. Primer Color Code.**

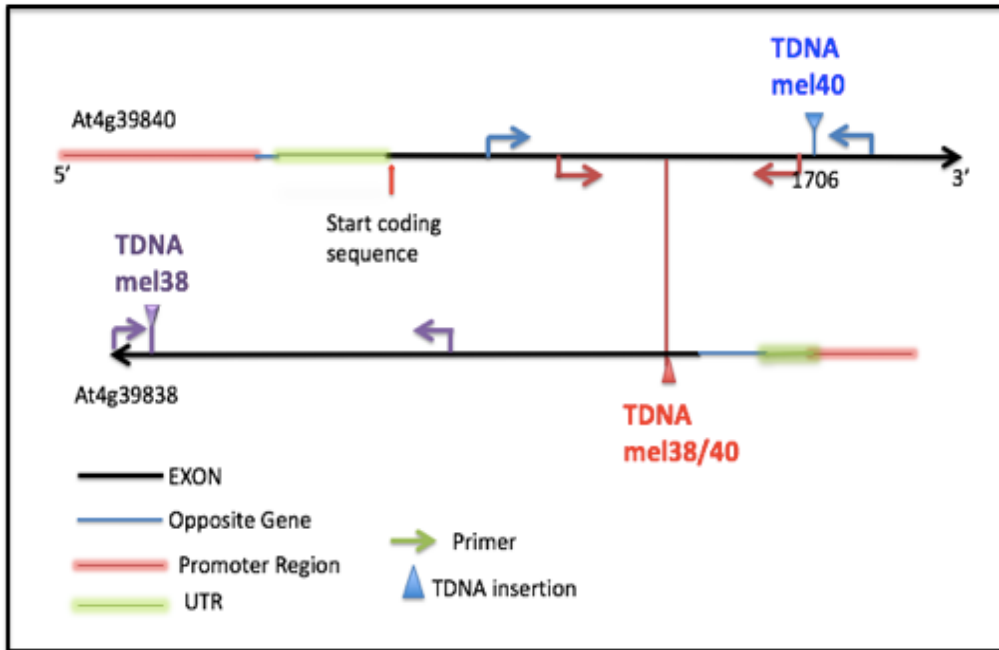
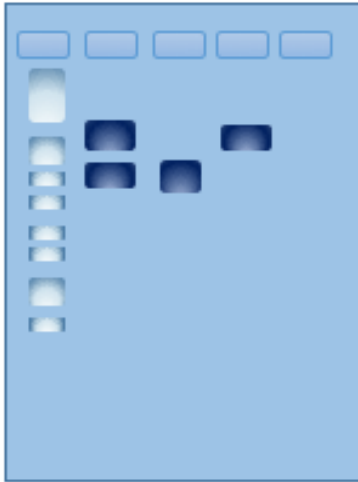


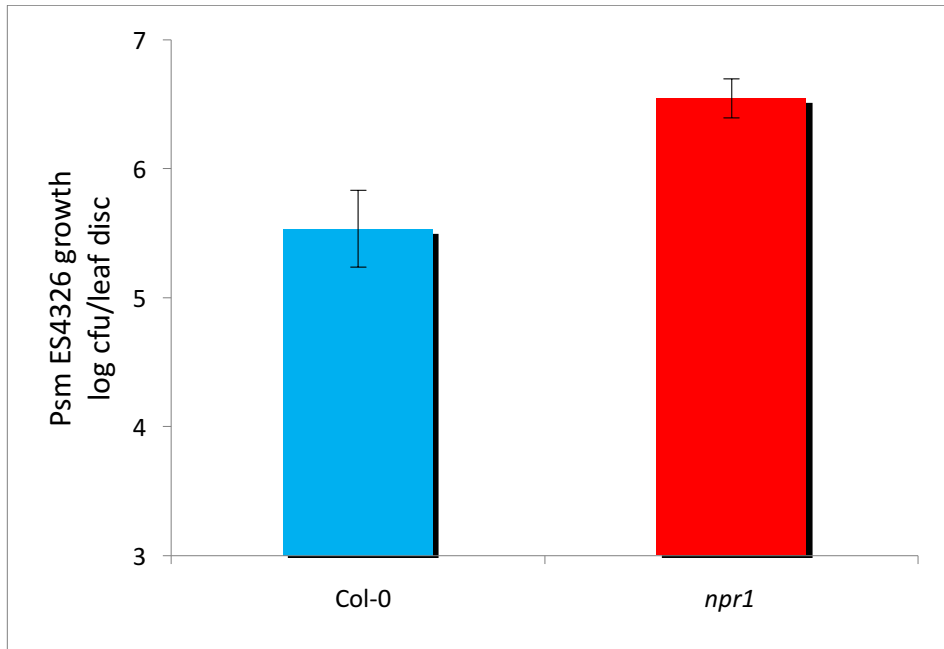
Figure S1. At4g39840/At4g39838 primer and T-DNA insertion design for miR5658



**Figure S2. Position key for genotyping gel.**

PCR analysis using gene specific primers showing heterozygosity, homozygosity for the mutant allele, and homozygosity for WT.

The bands on the left are considered your DNA ladder because they dictate the position of your DNA from the number of base-pairs it has. The second column has two bands next to each other, which means the DNA is heterozygous. The third column has one band at a lower position, indicating that this DNA is homozygous for the gene you want. Lastly, the fourth row has one band at a higher level, indicating that this DNA is merely WT. These results are a good indication that your genotyping PCR worked accurately. However, you must also determine quantitatively if your gene is in fact homozygous or heterozygous through a Real-Time quantitative PCR (RT-qPCR).



**Figure S3. Bacterial log growth quantification of Wild-type (WT) Col-0 and mutant plant *npr1*.**

*Psm ES4326* growth (colony forming units – cfu/leaf disc, expressed on a log scale) was quantified in four-week-old plants two days post syringe inoculation ( $OD_{600nm} = 0.001$ ). Error bars represent 95% confidence intervals of the mean ( $n = 1$ ). Experiments were repeated four independent biological replications with similar results. Analysis was conducted via quantification of bacterial growth on Kb-S media and converted to a graph for phenotypic comparison.

## Media

### KB media

1 L of King's B (KB) media requires 1 L of distilled water, 20 g of peptone, 2 g of  $K_2HPO_4 \cdot 3H_2O$ , 15 g of agar. This solution was autoclaved on a liquid cycle, allowed to cool and then 6.2 mL of 1M  $MgCl_2$  and 18 mL of 80% glycerol are added, along with required antibiotics (typically streptomycin at 50 mg/L).

### YEB media

1 L of YEB was made using 1 L of distilled water, 20 grams of proteose peptone #3, 2 grams of  $K_2HPO_4$ , 6.1 mL of  $MgCl_2$ , 18 mL of 80% glycerol and 15 grams of agar. This solution was autoclaved using a liquid cycle and allowed to cool before adding necessary antibiotics.

### MS media

Murashige and Skoog medium was prepared using a modified basal medium with Gamborg vitamins (PhytoTechnology Laboratories<sup>®</sup>). The medium contained the MS mix at 4.44 g/L dissolved in  $H_2O$  after which, pH levels were brought to 5.7-5.8 with KOH. Then, 6 g of sucrose along with 7 g of agar were added before autoclaving on a liquid cycle. The antibiotic ampicillin (50 mg/L) was used to prevent bacterial growth and added after media was cool to touch.

## LB media

Lysogeny broth was prepared using 950 mL of distilled water, 10 grams of tryptone, 10 grams of sodium chloride, and 5 grams of yeast extract. LB agar plates are made using the same recipe plus 15 grams of agar. The solution was mixed evenly and autoclaved using a liquid cycle. The mixture was allowed to cool before adding necessary antibiotics.